ECOLE POLYTECHNIQUE FEDERALE DE LAUSANNE
SCHOOL OF LIFE SCIENCES

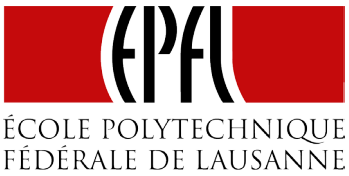

Master's project in Life Sciences and Technology

Expansion of a VE-Cadherin^{+}CD45^{+} population in the yolk sac upon Etv2 overexpression in the mouse embryo
-
Effects of BMP and Wnt signaling inhibition on the differentiation of a Flk1^{+} extraembryonic mesoderm *in vitro* model

Carried out in the Laboratory for Stem Cell Biology
at RIKEN Center for Developmental Biology, Kobe
Under the supervision of
Professor Shin-Ichi Nishikawa, MD, PhD, head of the lab

Done by
Matteo Pluchinotta

Under the direction of
PROF. Yann Barrandon
in the Laboratory of Stem Cells Dynamics
EPFL

LAUSANNE, EPFL 2011

Table of contents

1.	Abstract	**5**
2.	Introduction	**7**
3.	Materials and methods	17
4.	Results	**23**
5.	Discussion	**41**
6.	Acknowledgments	**45**
7.	Bibliography	**45**
8.	Abbreviations used	**52**

1. Abstract

The difficulty to find compatible donors for bone marrow transplantation makes the need for an alternative source of HSCs urgent. HSC derived from patient-specific iPS cells are ideal candidates for this purpose. Nevertheless, although HSCs are the best characterized adult stem cells, the *in vitro* generation and expansion of *bone fide* HSCs still has not been achieved without transgene insertion. Successful derivation of HSCs from ES cells or iPS cells will require a comprehensive understanding of inductive signals and downstream effectors involved in the normal arising of HSCs during embryonic development. BMP and Wnt signaling pathways play a very important role in this differentiation process. Here, we report how BMP and Wnt signaling inhibition cooperatively alter the differentiation of $Flk1^{+}PDGFR\alpha^{-}$ cells after reculture in serum-free, feeder layer-free conditions. This data will be useful in determining the factors that have to be added to a chemically defined culture medium aimed at derivation of *bone fide* HSC *in vitro*. In the second part of this master's project, we studied the spatial and temporal localization requirements of Etv2 expression, a key regulator of the earliest events in the development of the hematopoietic and vascular systems. To gain more insight on this matter, we conditionally knocked-in Etv2 in the early endothelial compartment, using a Tie2Cre system. This leaded to an embryonically lethal phenotype by E11.5, and most interestingly, to the expansion of a $VE\text{-}Cadherin^{+}CD45^{+}$ population in the E10.5 yolk sac. We believe that these cells represent a increased pool of immature pre-definitive hematopoietic stem cells, thus underlining further the importance of Etv2 in the differentiation process towards hematopoietic, and endothelial lineages in the mouse embryo.

Key words: Mater title - Specialization - Hematopoietic stem cell - Etv2/ER71 - Embryonic stem cell

2. Introduction

Embryonic Stem (ES) cells are derived from the inner cell mass of preimplantation or peri-implantation blastocysts. They were first isolated from mouse blastocysts in 1981.[1,2] ES cells have the ability to self-renew *in vitro*, to differentiate into tissues derived from all 3 embryonic germ layers (pluripotency) and to form teratomas when injected in immunodeficient mice. They also have the capacity to contribute to all tissues of chimeric mice, including the germ-line, upon microinjection into a host blastocyst.[3] ES cells can be maintained in an undifferentiated state by numerous cell intrinsic and environmental factors and can thus be cultured and expanded *in vitro*.[4,5] Differentiation into various tissue types can also be induced in vitro, including towards hematopoietic cells.[6,7] Direct reprogramming of mouse fibroblasts to induced pluripotent stem (iPS) cells by overexpression of four transcription factors (Oct4, Sox2, Klf4 and c-Myc) was achieved in 2006.[8] The following year, it was shown to be achievable with human cells as well,[9,10,11] permitting to derive patient-specific ES cell equivalents and opening new frontiers for regenerative medicine, disease modelling and drug discovery. Nowadays, iPS cells can be generated from various mouse, human, and other animals somatic cell types, using viral, non-viral or chemical methodologies.[12,13] iPS cells are now widely accepted as closely resembling ES cells in their morphological, molecular and developmental attributes, although they may not have identical global gene expression patterns[14] and epigenetic state.[15,16,17,18,19]

Repopulation of the entire hematopoietic system for extensive period of time can be achieved by the transplantation of a single hematopoietic stem cell (HSC) in a suitable adult host.[20] Those cells have thus an incredible potential to cure hematological disorders, and have been used to treat such diseases for over 40 years.[21,22] However, the difficulty to find compatible donors to carry out transplantation makes the need for an alternative source of HSCs urgent. HSC derived from patient-specific iPS cells are amongst the best candidates for these replacement cell therapies. However, although HSCs are the best characterized adult stem cells, and despite the fact that it is relatively easy to generate multipotent hematopoietic progenitors with extensive proliferative capacity from ES cells and iPS cells,[6,7,23] the generation and expansion of HSCs from ES-like cells that haven't been genetically modified remains a challenge;[24,25] most studies reported weak and inconsistent repopulation capacity after irradiation in transplantation assays.

Therefore, successful derivation of HSCs from ES cells or iPS cells will require a comprehensive understanding of inductive signals and downstream effectors involved in the normal arising of HSCs during embryonic development.

The developmental process of the hematopoietic system and signaling pathways that regulates it are generally conserved throughout vertebrate evolution, including humans. Embryonic hematopoiesis is generally divided in two parts: primitive and definitive. Primitive hematopoiesis is restricted to the yolk sac and starts around embryonic day (E) 7 in mouse. It gives rise to primitive erythrocytes, macrophages and megakaryocytes.[26,27] Definitive hematopoiesis occurs at different places and different times in the mouse conceptus: yolk sac, placenta, vitelline and umbilical arteries, and para-aortic splanchnopleura (P-Sp), which later contains the aorta, gonads and mesonephros (AGM). It starts at around E8, and gives rise to all blood lineages and ultimately to definitive HSCs at around E10.5.[26,27] The relative contribution of each of the above sites to the final pool of adult HSCs is still largely unknown. Within the AGM, HSCs emerge from an hemogenic endothelium located in the ventral wall of the dorsal aorta. [28,29,30,31,32]

The idea that hematopoietic cells and endothelial cells emerge from a common precursor was formulated for the first time more than 90 years ago by Florence Sabin, who observed the formation of blood islands from undifferentiated mesoderm in the yolk sac of the chick embryo.[33,34] She noted that these mesodermal cells differentiated into solid angioblastic cords of cells that had the potential to mature into endothelial cells, blood plasma, and primitive erythroids.[35] These observations were the seed to the idea that a common multipotential precursor, the hemangioblast, might exist for endothelial and hematopoietic lineages.[31,32,36] The existence of cells that have such potential has been proven *in vitro*,[23,37] and *in vivo*.[38] However, after decades of debate on the matter, a clear unifying definition of this precursor cell has is still missing. Our lab defends a hemogenic endothelium model that is a little different from the classical view on this developmental process. We believe that all hematopoietic precursor cells originate from extraembronic mesoderm cells, that migrate to the embryo proper, at around E7.5-E8.

In the mouse embryo, at the onset of gastrulation (around E6.5), the primitive streak is formed by epiblast cells from the posterior part of the embryo that undergo an epithelial to mesenchymal transition. The mesoderm emerges from the primitive streak and migrates away from it laterally and anteriorly. It will give rise to blood, endothelium, connective tissue, and skeletal, smooth and cardiac muscle. All nascent mesodermal cells express Brachyury (Bry).[39,40,41] Cells from the anterior regions of the primitive streak preferentially express Foxa2 and Goosecoid, when the ones from the posterior regions express HoxB1 and Evx1.[6] Epiblast cells that will give rise to the extraembryonic mesoderm, which forms the hematopoietic, endothelial and vascular smooth muscle cells of the yolk sac, allantois and amnion, are the first mobilized and traverse the posterior primitive streak. Generation of cranial, cardiac, paraxial and axial mesoderm occurs as gastrulation proceeds and cells migrate through more anterior parts of the primitive streak. Bone morphogenic protein 4 (BMP4), Nodal and members of the Wnt family are essential for those developmental steps.[6]

The subset of Bry-expressing (Bry^+) mesodermal cells that express Fetal liver kinase 1 (Flk1, Kdr, or Vascular endothelial growth factor receptor 2, VEGFR2) but not Platelet-derived growth factor receptor α (PDGFRα) will become proximal and extraembryonic mesoderm, the cells that express PDGFRα but not Flk1 will become paraxial mesoderm and the ones that express both

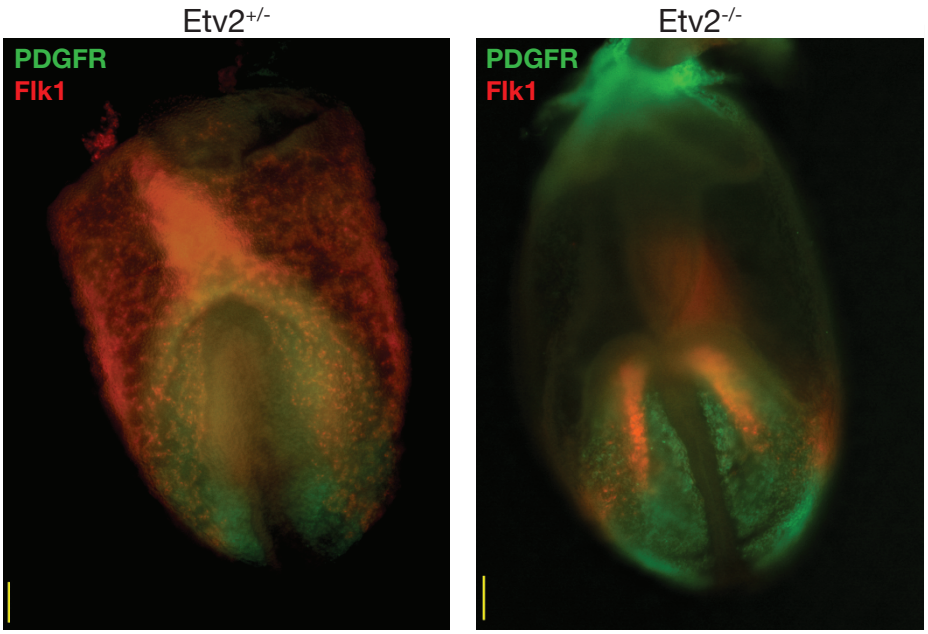

Figure 1. Flk1 and PDGFRα expression patterns in E7.5 mouse embryos
Immunostaining and fluorescence imaging of $Etv2^{+/-}$ and $Etv2^{-/-}$ E7.5 embryos. No $Flk1^+$ extraembryonic mesoderm formation in the full knockout embryo. PDGFRα expression is unaffected. 40x, scale bar = 100μm. Courtesy of Dr. Hiroshi Kataoka

represents a transient, undifferentiated multipotential population.[42,43,44] These double-positive cells eventually lose the expression of either Flk1 or PDGFRα and become single-positive cells. Flk1^{+}PDGFRα^{-} cells represents the population that we affirm have the potential to migrate towards the dorsal aorta at around E7.5-E8.0, and become angioblasts. Combined BMP, Notch and Wnt signaling is required for Flk1^{+} mesoderm formation.[45,46]

Flk1 is a receptor tyrosine kinase that binds Vascular endothelial growth factor (VEGF) with high affinity. It is a marker for extraembryonic mesoderm (which includes lateral plate mesoderm, yolk sac mesoderm), allantois, and cardiac crest.[47] (Fig. 1) Flk1 is necessary cell-autonomously for both endothelial and hematopoietic development, *in vitro* and *in vivo*.[48,49] *Flk1*$^{-/-}$ and *VEGF*$^{+/-}$ knockout mice display similar phenotypes: defects in the yolk sac blood islands, blood vessels, and endocardium. They die around E9.5, indicating that VEGF is one of the most important ligand of Flk1 during developmental hematopoiesis and angiogenesis and that this signaling is necessary for the establishment of both hematopoietic and vascular systems.[46] Despite its crucial role in the onset of hematopoiesis an generation of the circulatory system, the mechanisms of

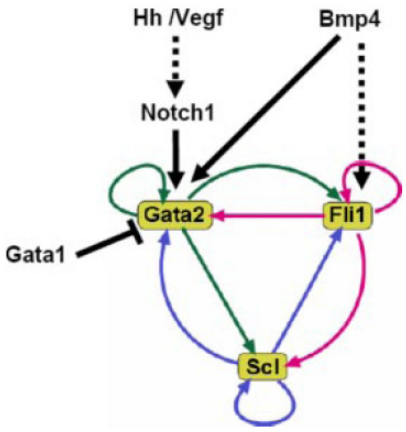

Figure 2. A fully connected triad of hematopoietic transcription factors
The GATA2/Fli1/Scl triad with putative initiators. Direct interactions are represented by solid lines, dashed lines represent indirect interactions. Copied from reference 50.

Flk1^{+} mesoderm formation and differentiation are still poorly understood. Extraembryonic mesoderm Flk1^{+} cells can give rise to both hematopoietic and endothelial lineages are can thus be considered as somehow equivalent to the conceptual hemangioblast. These cells may then activate a GATA2/Fli1/Scl recursively wired gene-regulatory circuit,[50] (Fig. 2) and differentiate both *in vitro* and *in vivo* into either definitive endothelial cells, or hemogenic endothelial cells.[23,37,38,51] Both endothelial cell types are marked by coexpression of the transcription factor Scl (also known as Tal1)[52], Tie2,[53,54] and Vascular endothelial cadherin (VE-Cad, also known as

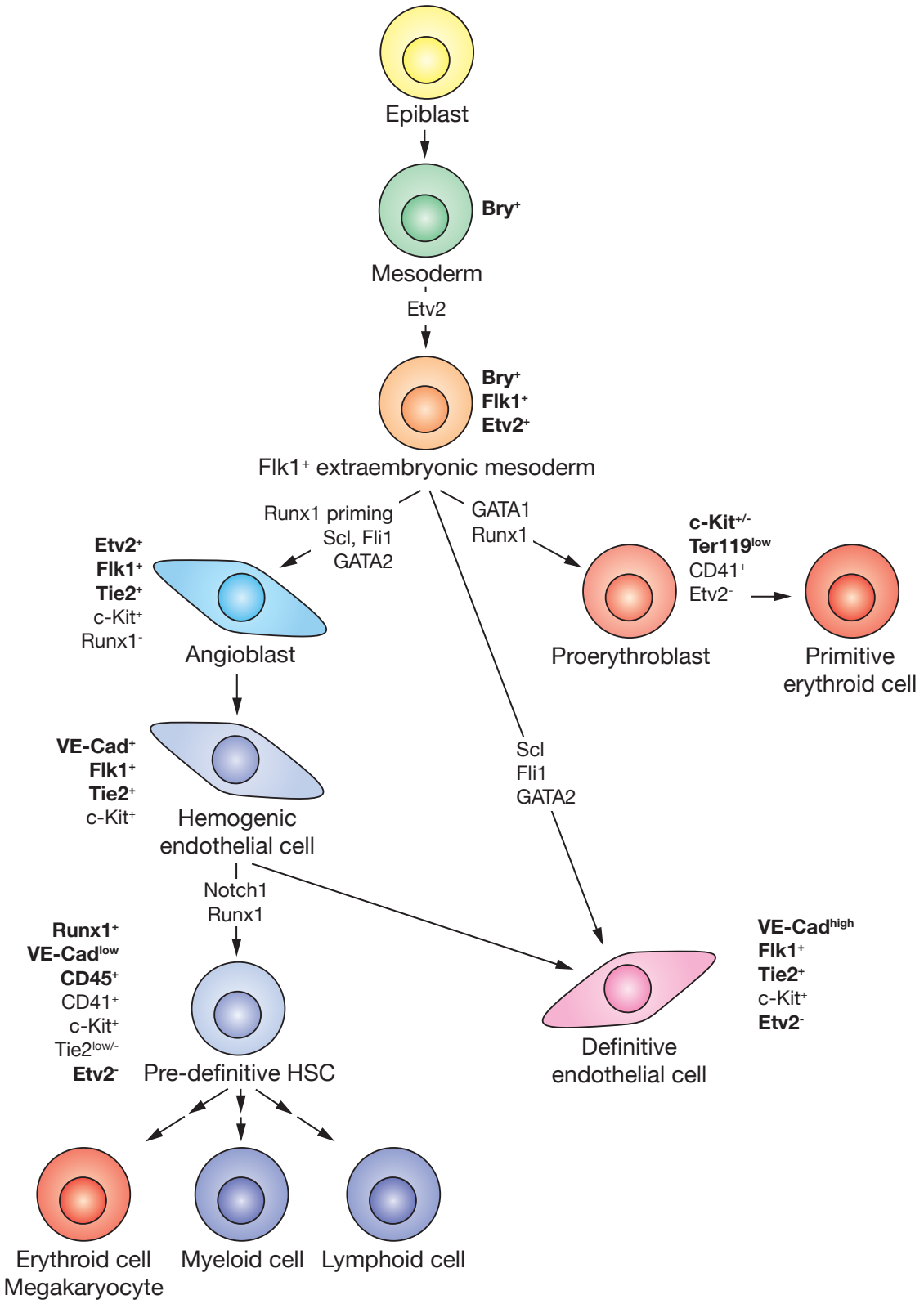

Figure 3. Model of blood cell formation from lateral plate mesoderm and yolk sac mesoderm
The specific phenotype of the cell populations, as well as the key regulators, transcription factors, or signaling pathways, involved in hematopoietic development are indicated.

Cdh5) expression.[51,55,56,57] These two cell types are distinguished by the fact that the hemogenic endothelial cells transiently expressed Runt-related transcription factor 1(Runx1, also called AML1) during their differentiation from Flk1$^+$ mesoderm.[58](unpublished data)

Flk1$^+$ extraembryonic mesoderm cells can also differentiate into proerythroblasts, which are early primitive erythroid progenitors that express GATA1 and are CD41$^+$Ter119$^+$c-Kit$^{low/-}$.[26,52,59,60] This process depends on Runx1 expression,[58,61,62] and is supposed to require Wnt signaling.[59]

Hemogenic endothelial cells were named this way because of their potential to differentiate into hematopoietic cells, or definitive endothelial cells. [26,38,63,64] CD41 is the earliest marker for hematopoietic differentiation.[65] Differentiation towards pre-definitive-HSC cells, which are Runx1$^+$VE-Cad^{low}c-Kit$^+$CD45$^+$, depends on Notch signaling.[26,52,38,59,66,67].(Fig. 3) The key transcription factor implicated in this process is Runx1, which is required for the transition from endothelial to hematopoietic cell.[68] Virtually all adult hematopoietic cells are derived from Runx1-expressing cells.[26,69] *Runx1*$^{-/-}$ mice die around E12.5 from a lack of definitive hematopoiesis, although they display almost normal primitive hematopoiesis.[62,70] There is rising evidence that Runx1 also has a major role in priming Flk1$^+$ extraembryonic mesoderm cells: Runx1$^+$Gata1$^-$ cells would become hemogenic endothelial cells, Runx1$^-$Gata1$^-$ cells appear to be fated towards definitive endothelial lineage, and Runx1$^+$Gata1$^+$ cells seem to be directed towards

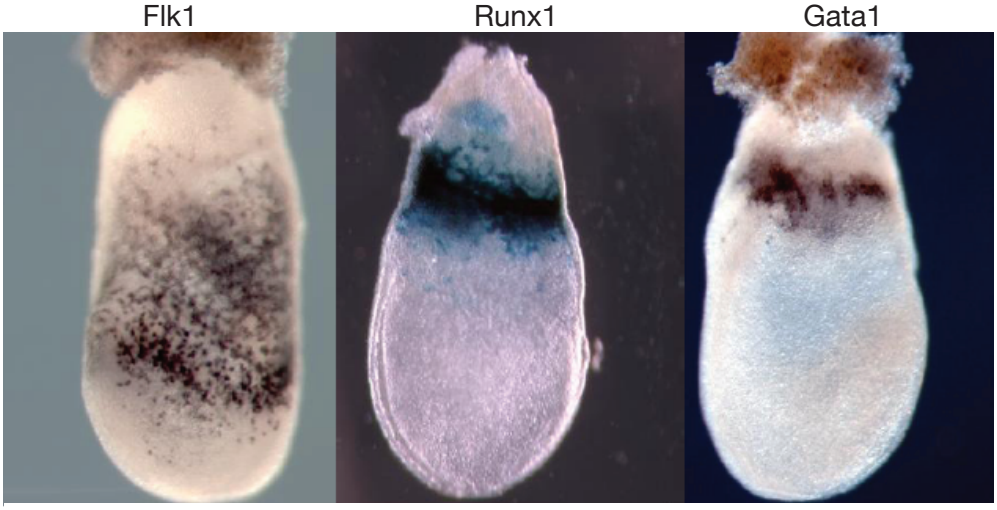

Figure 4. Expression pattern of Flk1, Runx1, and Gata1 in the E7.5 mouse embryo
Immunohistochemistry staining shows that Flk1 is broadly expressed in the whole extraembryonic mesoderm. β-Gal staining of a Runx1$^{LacZ/Wt}$ shows that Runx1 expression is limited to the proximal yolk sac at that stage. Gata1 expression is restricted to the blood isalnds at E7.5, as shown by immunohistochemistry. Courtesy of Professor Shin-Ichi Nishikawa

primitive erythropoiesis.[58,61,62] (unpublished data) Thus, the localization of the cells within the Flk1$^+$ extraembryonic mesoderm plays a major role in the differentiation pattern towards one of these three fates: at E7.5, Gata1 expression is limited to the blood island region, and Runx1 expression to the proximal yolk sac. (Fig. 4)

BMPs are members of the Transforming growth factor- β (TGF- β) superfamily of ligands. They induce type I and type II serine-threonine kinase receptors association. ALK2, -3, and -6 are the Type I receptors responsive to BMPs. Type II receptors then phosphorylate and activate type I serine-threonine kinase receptors, which in turn phosphorylate two Receptor-activated Smad proteins (R-Smads: Smad1, -2, -3, -5 or -8), which bind the Common-Smad (Co-Smad), Smad4. Smad1, -5, and -8 are implicated in BMP signaling, when Smad2, and -3 are implicated in TGF-β signaling. The trimeric Smad complexes then translocates to the nucleus, where they interact with other transcriptional regulators to control expression of target genes.[71,72,73,74,75] (Fig. 5)

BMP4 is essential during mouse embryonic development for gastrulation and mesoderm formation, as BMP4 -deficient mice are embryonic lethal due to severe mesodermal defects.[76] It has been shown that BMP4 induces the formation of Flk1$^+$ and hematopoietic cells in *in vitro* cell cultures,[43,77] and to activate hematopoietic transcription factors such as Runx1 and Gata2.[78,79,80] (Fig. 3) It has been suggested that BMP signaling plays a two-step role during ESC differentiation towards the hematopoietic lineage: it mediates dorsoventral patterning and induces ventral-posterior mesoderm at first, and then promotes blood specification from preformed mesodermal cells, possibly by upregulating Runx1 transcription.[79,26,81] BMP is supposed to be induced in those cells through Indian hedgehog (Ihh) signaling coming from the visceral endoderm.[32,82] On the other hand, there is rising evidence that BMP signaling plays a dual role in hematopoietic differentiation, *in vitro* at least; it has been shown Smad1 depletion before Flk1 expression limits the hematopoietic potential is limited due to a block in mesoderm development, but if Smad1 depletion occurs after Flk1$^+$ mesoderm commitment, the pool of hematopoietic progenitors is expanded.[83,84]

Wnt signaling has been demonstrated to be essential during gastrulation, to the formation of the primitive streak.[85,86,87] Wnt signaling is also implicated in this hematopoietic differentiation

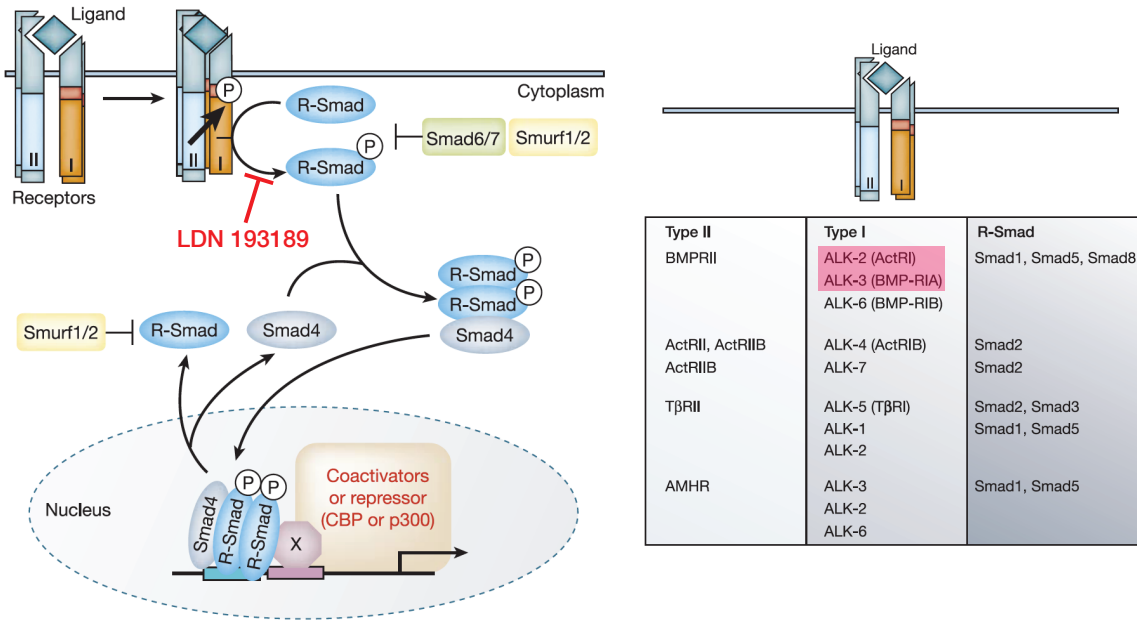

Figure 5. General mechanism of TGF-β signaling pathway
At the cell surface, the ligand binds a complex of transmembrane receptor serine/threonine kinases (types I and II) and induces transphosphorylation of the type I receptor by the type II receptor kinases. The activated type I receptors phosphorylate R-smads then form a complex with Smad4. Activated Smad complexes translocate into the nucleus, where they regulate transcription of target genes, through physical interaction and functional cooperation with DNA- binding transcription factors. Activation of R-Smads by type I receptor kinases is inhibited by Smad6/7. The E3 ubiquitin ligases Smurf1/2 mediate ubiquitination and consequent degradation of R-Smads. LDN 193189 inhibits ALK-2, and -3, preventing phosphorylation, and activation of Smad1/5/8 (red arrow and box). Adapted from reference 72.

process.[88] It promotes differentiation towards blood fate through the activation of the Cdx-Hox genetic pathway: Cdx1 and Cdx4 are direct targets of the canonical Wnt pathway.[89,90] Those genes in turn activate *Hox* genes such as *HoxB4*, which have been shown to be related to the expansion of the hematopoietic cell pool.[79,91,92,93,94,95] What is more, Wnt and BMP signaling have been shown to cooperate in the specification of hematopoietic fate; BMP activates the Cdx-Hox pathway through the Wnt effector LEF1.[46,79]

In the presence of Wnt, binding of Wnt to its receptor, Frizzled (Fz), leads to the stabilization of cytoplasmic β-catenin: Fz forms a complex with LRP5/6, and recruits Dishvelled (Dvl). Dvl phosphorylates LRP5/6, leading to the recruitment of Axin. This disrupts the phosphorylation/degradation of β-catenin mediated by the Axin complex (Axin, APC, GSK3, and CK1). In turn β-catenin translocates to the nucleus, where it can activate the transcription of its target genes, after association with Lef/TCF transcription factors. In the absence of Wnt, cytoplasmic β-catenin is sequestered by the Axin complex. CK1, and subsequently GSK3, phosphorylate β-catenin and target it for proteosomal degradation upon recognition by the E3 ubiquitin ligase β-Trcp.

In the absence of β-catenin, Wnt target genes are repressed by the TCF-TLE/Groucho complex and Histone deacetylases (HDACs). CK1 also phosphorylate Axin and APC and enhance their binding to β-catenin and degradation complex stability. APC facilitates Axin degradation and possibly vice versa. PP1 dephosphorylates Axin to antagonize CK1 phosphorylation and

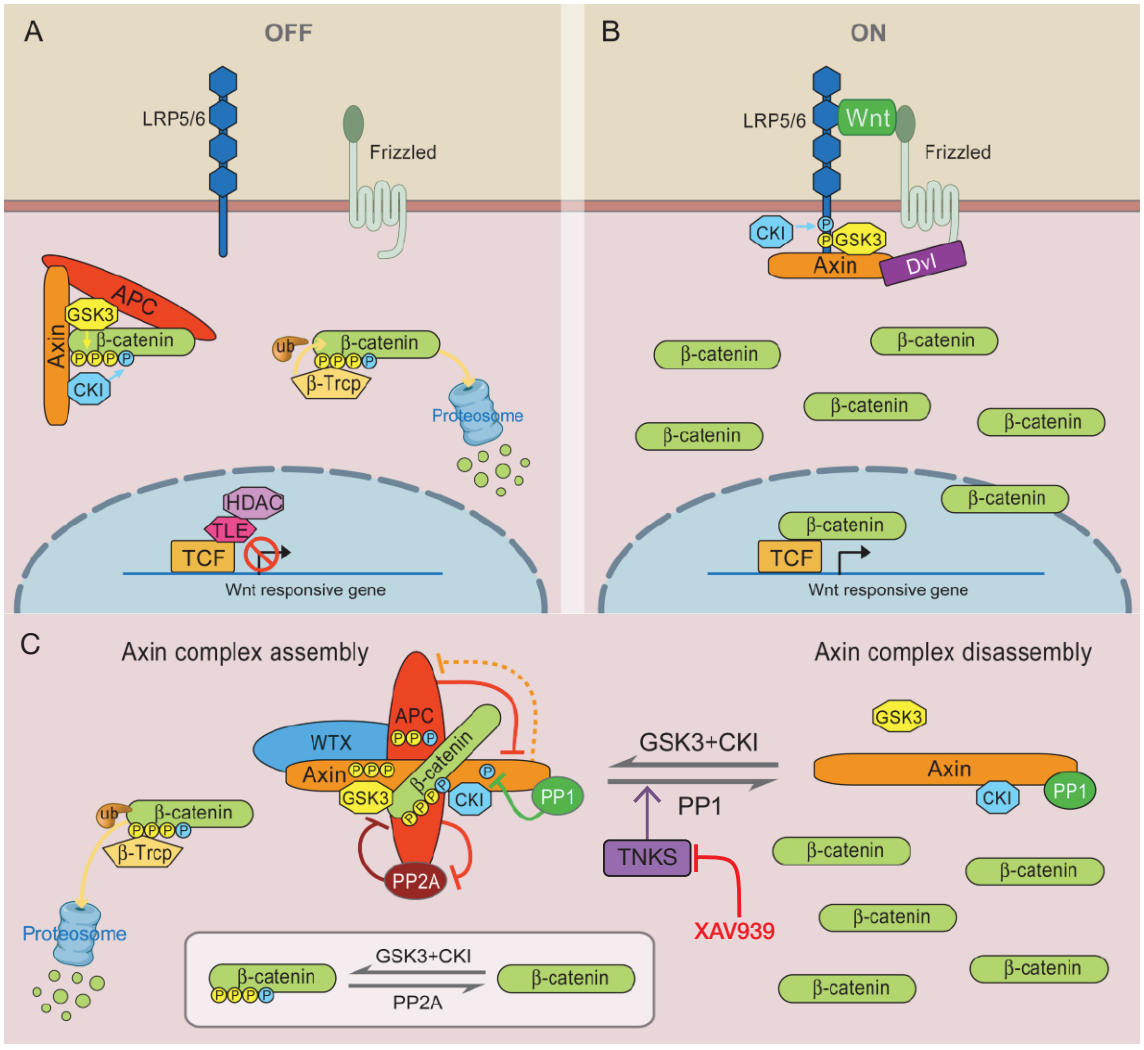

Figure 6. General mechanism of the Wnt signaling pathway
A In the absence of Wnt, cytoplasmic β-catenin forms a complex with Axin, APC, GSK3 and CK1, and is phosphorylated by CK1, and subsequently by GSK3. Phosphorylated β-catenin is targeted for proteosomal degradation upon recognition by the E3 ubiquitin ligase β-Trcp. Wnt target genes are repressed by the TCF-TLE/Groucho complex and HDACs. **B** In the presence of Wnt ligand, a receptor complex forms between Fz and LRP5/6. Dvl recruitment by Fz leads to LRP5/6 phosphorylation, and Axin recruitment. This disrupts Axin-mediated phosphorylation/degradation of β-catenin, allowing β-catenin to accumulate in the nucleus where it serves as a co-activator for TCF to activate Wnt responsive-genes. **C** The core components of the Axin complex, Axin, APC, GSK3 and CK1 collectively promote β-catenin phosphorylation for degradation by β-Trcp. GSK3 and CK1 also phosphorylate Axin and APC and enhance their binding to β-catenin and degradation complex stability, further ensuring β-catenin phosphorylation. APC may also act to prevent PP2A dephosphorylation of β-catenin. APC facilitates Axin degradation and possibly vice versa. PP1 dephosphorylates Axin to antagonize CK1 phosphorylation and negatively regulates GSK3-Axin binding resulting in complex disassembly. Tankyrase (TNKS) destabilizes the Axin complex by stimulating its degradation through the ubiquitin proteasome pathway, thus promoting the activation of the Wnt-responsive genes. XAV939 inhibits TNKS, and thus stabilizes the Axin complex and inhibits Wnt-responsive gene activation. Adapted from reference 96.

negatively regulates GSK3-Axin binding, resulting in complex disassembly. Tankyrase (TNKS) destabilizes the Axin complex by stimulating its degradation through the ubiquitin proteasome pathway, thus promoting the activation of the Wnt-responsive genes. [89,96] (Fig. 6)

In the first part of this project, in order to better characterize the requirement for BMP and Wnt signaling in endothelial and hematopoietic differentiation, we used small molecule inhibitors to inhibit these two signaling pathways in an ES cell differentiation system modeling Flk1$^+$ extraembryonic mesoderm, in serum free, layer free conditions.[97,98,99] The data we accumulated indicates that although both BMP and Wnt signaling play a role in this differentiation process, none of them seems to be absolutely required to obtain endothelial and/or hematopoietic cells. Furthermore, our data partly reproduces what was observed in the Smad1 knockout experiment.[84]

Ets variant 2 (Etv2 also called ER71) is a transcription factor of the ETS family that has a non-redundant and indispensable function in the regulation of blood and vessel development during mouse embryogenesis. It is expressed mainly in Flk1$^+$ mesoderm and its derivatives. *Etv2*$^{-/-}$ mice are embryonically lethal; embryos die around E9.5 from failure to develop blood, vessels, and endocardium.[46,100] In these embryos, no Flk1$^+$ extraembryonic mesoderm could be detected. (Fig. 1) In *Etv2*$^{-/-}$ ESC cultures, approximately the same phenotype was observed. (unpublished data) Thus showing that Etv2 is absolutely required for the formation of Flk1$^+$ cells and for the development of blood and endothelial cells in embryos and in *in vitro* cultures. Etv2 expression is lost upon differentiation towards committed hematopoietic cell, or definitive endothelial cell fate. In zebrafish, Etv2 ortholog Ets-related protein (Etsrp) has been shown to be necessary for early embryonic vasculogenesis and hematopoieis.[101] It functions downstream of a network combining BMP, Notch and Wnt signaling and regulates the expression of Flk1.[32] Our hypothesis is that Etv2 switches on the GATA2/Fli1/Scl recursively wired gene-regulatory circuit during early hematopoietic development.[78,102] This seems to be the case, as overexpression of either Scl or Fli1 in *Etv2*$^{-/-}$ ESCs can rescue these cell's incapacity to differentiate into hematopoietic cells. (unpublished data) In *in vitro* cultures, it has been shown, using inducible Etv2 ESCs that overexpression of Etv2 in ESCs leads to the induction of Flk1$^+$ extraembryonic mesoderm-like cells.[46]

Tie2 (also called Tek) is a tyrosine receptor kinase that binds angiopoietins. Its expression starts at E7.5 in endothelial precursor cells, and angioblasts. Its expression is kept during development and throughout adulthood in virtually all endothelial cells.[103,104,54,105] Hematopoietic precursor cells have been shown to express Tie2 as well, thus Tie2 expression spans the transition from angioblast to hemogenic endothelial cells.[53,106] *Tie2*$^{-/-}$ mice die *in utero* from severe vascular defects, indicating that it is required for maintenance and organization of endothelial cells into a functional vasculature during development.[107] It is thus a marker of choice for the study of pan-endothelial processes during embryonic development.

To gain more insight on the *in vivo* importance of the spatial and temporal localization of the Etv2 signal during the early development. Overexpressing Etv2 in the Tie2 compartment, using a conditional knockout mouse, we were able to demonstrate that Etv2 expression is required to be transient; artificially maintaining Etv2 expression in the hematopoietic and endothelial compartments results in embryonic lethality at around E11.5.

3. Materials and Methods

Embryo generation

Mating of adult Tie2-Cre$^{WT/Tg}$ males with Rosa26-etv2-IRES-GFP$^{Tg/Tg}$ females was carried out overnight. Time-pregnant mice were killed by CO_2 inhalation and uteri with embryos were removed by dissection. Pictures of the embryos were taken with a Keyence Biorevo inverted microscope. Contrast of the pictures was modified using Photoshop CS5 (Adobe).

PCR genotyping

Mice were genotyped using samples extracted either from embryo yolk sac or from adult mouse tail. The samples were lysed at 55°C with 200µg/mL ProK for 2-3h. Lysis was stopped by heat-inactivation at 95°C for 10min. PCR reaction mix included sample DNA 1:20, KOD-Fx buffer (Toyobo), autoclaved MilliQ DEPC-treated H_2O, dNTP mix (2mM each, Toyobo), KOD-Fx polymerase (Toyobo) and primers (*ROSA26* locus: R1295: 5'-gcgaagagtttgtcctcaacc-3', R523: 5'-ggagcgggagaaatggatatg-3', R26F2: 5'-aaagtcgctctgagttgttat-3'; *etv2GFP*: Venus S11: 5'-gtacaactacaacagccacaacgtc-3', Venus AS11 5'-cacgaactccagcaggaccatgtg-3'; *Tie2Cre*: Cre Rev2: 5'-agtgcgttcgaacgctagagcctg-3', Tie2 5'F: 5'-gtgctcagacagaaatgagactg-3'). The reaction consisted

in 5 cycles at 58°C followed by 31 cycles at 56°C (33 cycles for embryo DNA samples). The reaction was carried out using a GeneAmp PCR System 9700 (AB). Reaction products were then mixed with loading buffer 1x (TaKaRa) and loaded on 2% agarose gels containing 0.5mg/mL ethidium bromide. Gel-electrophoresis was performed (20min, 130V) and imaging was done with a printograph.

Cell culture

OP9 feeder layers were prepared in T25 or T75 culture flasks (Falcon), or 12-well tissue culture-treated plates. OP9 cells were cultured in α-minimal essential medium (αMEM) (GIBCO) supplemented with 20% fetal calf serum (FCS) (JRH, batch #3G0267). Every 3 days, OP9 cells were dissociated by a 3min trypsin/EDTA 0.05% treatment at 37°C and split threeways. CCE mouse ES cells were maintained in knock-out Dulbecco's modified Eagle's medium (KO-DMEM) (GIBCO) containing 15% FCS (JRH, batch #4J0511), 1x non-essential amino acids (NEAA) (GIBCO), 2mM L-Glutamin (GIBCO), 10^{-4} M 2-mercaptoethanol (2-ME) and 10^3 U/mL leukemia inhibitory factor (LIF) (Chemicon). CCE cells were seeded on gelatine (SIGMA)-coated 6cm tissue culture-treated dishes (Falcon) and were passaged every 2 days: after a 3min trypsin-mediated dissociation using trypsin/EDTA 0.25%, $2x10^5$ cells were seeded on a new gelatine (SIGMA)-coated 6cm culture dish. OP9 and CCE cells were incubated at 37°C, 5% CO_2 and 95% humidity. OP9 and CCE cells were not cultured for more than 20 passages. All mediums contained 50U/50µg/mL penicillin/streptavidin (Meiji). Pictures of the cell cultures were taken with a Leica DMI 4000B inverted microscope, and the Leica FIRECAM v3.3.1 software (Leica). Contrast of the pictures was modified using Photoshop CS5 (Adobe).

ES cell differentiation

To induce differentiation, CCE cells were seeded at density of 2400 cells/cm^2 on confluent OP9 feeder layers, in either T25 or T75 culture flasks, in αMEM containing 10% FCS (Multister, batch #C10031) and $5x10^{-5}$ M 2-ME, in the absence of LIF. They were then incubated at 37°C, 5% CO_2 and 95% humidity. After 4 days for ES cell differentiation, cultured cells were harvested: floating cells were collected, adherent cells were dissociated with a 3min trypsin/EDTA 0.05% (GIBCO) treatment, and replated for at least 30min to let the OP9 cells become adherent. The floating cells so-obtained were added to the ones collected in the first place. The harvested cells were left to recover in αMEM containing 10% FCS (Multister, batch #C10031) and $5x10^{-5}$

M 2-ME for 30 min before being stained and sorted. All mediums contained 50U/50µg/mL penicillin/streptavidin. Pictures of the cell cultures were taken with a Leica DMI 4000B inverted microscope, with the Leica FIRECAM v3.3.1 software (Leica). Contrast of the pictures was modified using Photoshop CS5 (Adobe).

Preparation of single cell suspensions from E10.5 embryos

Pregnant female mice were dissected 10.5 days post-coitum (dpc). Embryo proper and yolk sac were separated by dissection, and kept separated thereafter. They were washed in PBS and incubated 10min in trypsin/EDTA 0.05% at 37°C. Trypsinization was stopped with stop-solution (Hank's balanced salt solution (HBSS) (GIBCO) containing 5mg/mL DNaseI (QIAGEN), 20% FCS and CaCl2 10^{-4}M), and the embryos were dissociated by pipetting. Finally, cells were resuspended in αMEM containing 10% FCS (Multister, batch #C10031) and $5x10^{-5}$ M 2-ME, and left to recover for 30 minutes at 37°C, 5% CO_2 and 95% humidity.

Flow cytometry and cell sorting by Fluorescence-activated cell sorting (FACS)

Harvested differentiated ES cells were washed two times in Hank's balanced salt solution (HBSS) (GIBCO) containing 1% bovine serum albumin (BSA, SIGMA), before being blocked in HBSS containing 1% BSA and 10% mouse serum for 30min at 4°C. Direct staining was achieved by incubation with Phycoerythrin (PE)- conjugated Flk1 (AVAS12a1, eBioscience) and Allophycocyanin (APC)-PDGFRα (CD140a) (APA5, eBioscience) monoclonal antibodies (MoAbs) for 15min on ice. The cells were washed three times with HBSS containing 1% BSA. Living $Flk1^{+}PDGFR\alpha^{-}$ cells were sorted and recultured in layer- and serum-free conditions. After 4 days of culture, the cells were harvested and analyzed using the following conjugated MoAbs , using CD41-PE-Cy7 (eBioMWReg30, eBioscience), c-Kit (CD117)-PE (ACK2, eBioscience), CD11b-Fluorescein Isothiocyanate (FITC) (M1/70, BD), CD45-APC (30-F11, BD), CD45-FITC (30-F11, eBioscience), CD105-eFluor 450 (MJ7/18, eBioscience), Tie2-PE (TEK4, eBioscience), VE-Cad-PE-Cy7 (VECD1, Biolegend), and Ter119-eFluor 450 (TER119, eBioscience). The staining was done using the same protocol as mentioned above.

Single cell suspension from embryos were stained and analyzed following the same protocol, with different combinations of conjugated MoAbs: VE-cad-PE-Cy7 (VECD1, Biolegend), CD45-APC (30-F11, BD), c-Kit-PE (ACK2, eBioscience), Tie2-PE (TEK4, eBioscience), and

CD41-PB (eBioMWReg30, eBioscience). The FITC channel was used to detect the GFP signal from the transgene.

The cells from the B-cell assay were stained following the same protocol, with a different combination of conjugated-MoAbs: B220 (CD45R)-APC (RA3-6B2, eBioscience), CD19-PE (1D3. BD), VE-Cad-PE-Cy7 (VECD1, Biolegend), c-Kit-PE (ACK2, eBioscience), and CD45-APC (30-F11, BD).

In all FACS experiments, cells were gated to exclude small debris, dying cells and other sources of background interference and propidium iodide (PI)-gated to discard dead cells. These experiments were performed using a FACSAria II Special Order System (BD) with FACSDiva v6.1.3 software (BD). Data was analyzed using the FlowJo software v9.3 (Tree Star).

Cell reculture after FACS

$Flk1^{+}PDGFR\alpha^{-}$ cells were recultured in collagen-IV-coated 6-well plates (BD Biocoat) or in collagen-I-coated 4-well culture-slides (BD Biocoat), at a density of $3.125x10^{4}$ cells/cm^{2}, in SFO3 medium (Sankojunyaku) containing $5x10^{-5}$ M 2-ME, 100π/mL mouse Interleukin (mIL)-3 (purified in the lab), 100ng/mL granulocyte-colony-stimulating factor (G-CSF, Kirin), 100ng/mL stem cell factor (SCF, purified in the lab), and 100ng/mL recombinant human Erythropoietin (rhEPO, PROSPEC) or 10ng/mL recombinant mouse Erythropoietin (rmEPO, R&D). Cells were cultured in the presence or absence of BMP signaling inhibitor LDN-193189 (Stemgent), Wnt signaling inhibitor XAV-939 (Tocris), in duplicate. After 4 days incubation at 37°C, 5% CO_2 and 95% humidity,cells were harvested and analyzed by flow cytometry, or immunostained for fluorescence imaging.

$VE\text{-}Cad^{+}CD45^{+}$ cells isolated from E10.5 embryos were recultured on tissue culture-coated 12-well plates containing a confluent OP9 feeder layer, 500 cells/well, in 1mL of αMEM containing 10% FCS (JRH, batch #3G0267), $5x10^{-5}$ M 2-ME, 10ng/mL Flt3l (), 10ng/mL mIL-7 (), and 20ng/mL SCF. After 7 days incubation at 37°C, 5% CO_2 and 95% humidity, 1mL of the same medium, without the SCF was added to each culture well. On day 14 or 15, the cells were harvested following the same protocol as for the ES cell differentiation, and analyzed by flow cytometry.

All mediums contained 50U/50µg/mL penicillin/streptavidin.

Colony-forming unit (CFU) assay

Sorted VE-Cad$^+$CD45$^+$ cells isolated from E10.5 embryos were used in this assay. Cells were resuspended in αMEM containing 10% FCS (JRH, batch #3G0267) and 5x10^{-5} M 2-ME, at a concentration of 500 cells/100µL. 2000 cells were then mixed together with 4mL MethoCult GF M3434 (STEMCELL technologies) by vortexing. The tube was then left to rest for 5 minutes to allow bubbles to dissipate. 1.1mL of this cell suspension was dispensed in a 35mm Petri dish (Falcon). Each assay was done in triplicate. The three Petri dishes, plus a fourth one filled with sterile water, were kept in a square bacterial box for 8 days at 37°C, 5% CO_2 and 95% humidity. Burst-forming unit-erythroid (BFU-E), CFU-granulocyte (G), CFU-macrophage (M), CFU-granuolcyte, macrophage (GM), and CFU-granulocyte, erythroid, macrophage, megakaryocyte (GEMM) were counted on day 8. Pictures of the colonies were taken with a Leica DMI 4000B inverted microscope, with the Leica FIRECAM v3.3.1 software (Leica). Contrast of the pictures was modified using Photoshop CS5 (Adobe).

Immunostaining

After 4 days, Flk1$^+$PDGFRα$^-$ cells recultured on Collagen-I-coated 4-well culture slides were immunostained. Adherent cells were fixed in ice-cold methanol for 8min on ice. They were rehydrated through the ethanol serie (70%, 50% and 25%) and washed with phosphate-buffered saline (PBS). Blocking was achieved through incubation in PBS containing 2% skim milk (GIBCO) and 0.1% Tween 20 (Nacalai Tesque) (PBS-MT) 30min at room temperature (RT). The fixed wells were incubated with goat anti-ICAM2 (1/500, R&D), and rat anti-PECAM-1 (1/500, 390, BD) MoAbs overnight, on shake at 4°C. The wells were then incubated with Alexa-488-conjugated donkey anti-rat-IgG (1/500, Invitrogen) and Alexa-546-conjugated donkey anti-goat-IgG (1/500, Invitrogen)MoAbs overnight, on shake at 4°C. After each step, cultured cells were washed 3 times with PBS-MT. Finally, they were rinsed twice with PBS containing 0.1% Tween 20, and pictures were taken with a Keyence Biorevo BZ 9000 inverted microscope, with the manufacturer's software, BZ II (Keyence). Contrast of the pictures was modified using Photoshop CS5 (Adobe). Image overlays were done with the BZII software (Keyence).

The same protocol was applied to E9.5 mouse embryos, in a 24-well plate, except that the blocking was carried out for 6h on ice, and that the secondary antibody was incubated for 1h30min at RT, on shake. Primary antibody: goat anti-Flk1 MoAb (1/500, R&D), secondary antibody: Alexa546-conjugated donkey anti-goat-IgG MoAb (1/500, Invitrogen) .

RNA extraction

RNA was extracted using QIAGEN's RNeasy Micro Kit, following the manufacturer's protocol (Total RNA purification from animal or human cells, RNeasy MicroHandbook, 2nd edition, 12.2007). For the $Flk1^+$ recultured cells, RNA was extracted from 105 cells, for the microarray analysis from E10.5 VE-Cad^+CD45^+ cells, a few thousand cells were used in each reaction. In every case, cells were homogenized by one minute vortexing after resuspension in RLT buffer (QIAGEN).

Quantitative reverse transcriptase-PCR (qRT-PCR)

Reverse transcription was carried out using Toyobo's ReverTra Ace qPCR RT Kit, following the manufacturer's protocol. 50ng RNA was used for each reaction. Real-time PCR was performed in 25µL reactions consisting of 12.5µL Power SYBR Green PCR Master Mix (2x) (AB), 2.5µL primer mix (2µM each, Hokkaido System Science), and 100ng or 50ng of cDNA diluted in 10µL MilliQ DEPC-treated H_2O. Transcript levels were assessed using the 7500 Real Time PCR System (AB). The thermocycling conditions used were 2min at 50°C, 10min at 95°C, followed by 40 cycles of 15sec at 95°C, 1min at 60°C. At the end of the run, a thermal dissociation stage was added to assess the specificity of the polymerase reaction: 2 cycles of 15sec at 95°C, and 1min at 60°C. Data acquisition was done with the 7500 System Software (AB). Each experiment was done in triplicate. Gene expression analysis was performed using the Relative Standard Curve Method, using the housekeeping gene GAPDH for normalization.

Gene	Forward (5'-3')	Reverse (5'-3')
Runx1	CCAGGTAGCGAGATTCAACGA	CAACTTGTGGCGGATTTGTAAA
Gata2	GGCGTCAAGTACCAAGTGTCAC	CTCCCGGCCTTCTGAGCAGGAG
Fli1	TGCTGTTGTCGCACCTCAGTTA	TGTTCTTGCCCATGGTCTGTG
Scl	CAGCCTGATGCTAAGGCAAG	AGCCAACCTACCATGCACAC
Lyl1	CAGGACCCTTCAGCATCTTC	ACGGCTGTTGGTGAACACTC
Lmo2	TCAGCTGTGACCTCTGTGG	CACCCGCATCGTCATCTC
PU.1	TGTTACAGGCGTGCAAAATG	TCATGCATTGGACGTTGGTA
Erg	GGAGTGCAACCCTAGTCAGG	TAGCTGCCGTAGCTCATCC
Myb	AACGAGCTGAAGGGACAGCA	TGGCATGGTGTTCTCCCAAA
Gata1	AATCCTCTGCATCAACAAGC	GGAAGTGGAAGAAGATGCTG
Klf1	CCCTCCATCAGTACACTCACC	AGGGTCCTCCGATTTCAGAC
Sox17	CAGAACCCAGATCTGCACAA	GCTTCTCTGCCAAGGTCAAC

Table 1. qRT-PCR primer sequences

Microarray analysis

Microarray analysis was performed by the Genome Resource and Analysis Subunit of RIKEN CDB. At least 10ng of starting RNA were used for each sample. SurePrint G3 Gene Expression Microarrays - 8x60K (Agilent) were used. After scanning, digitalization was made with Feature Extraction10.7.3.1, and the data was analyzed using GeneSpring GX 11.5.1. The expression levels were first normalized, then the values for the Cre^+ samples were averaged, and compared to the value for the Cre^- control.

Statistics

Statistical analysis on the flow cytometry analysis data was performed using both regular and Bonferroni-corrected double-tailed, paired Student's t-test. Results were considered significant when p-value<0.05.[108]

4. Results

Effects of BMP and Wnt signaling inhibition on the differentiation of a $Flk1^+$ extraembryonic mesoderm in vitro model

It has been shown that BMP signaling, and Wnt signaling have an enhancing role at various time points of the differentiation process towards hematopoietic and endothelial fates, through the action of BMP4, and Wnt3a particularly.[74,76,79,82,85,88,89,90,91] In order to better characterize the requirement for BMP and Wnt signaling in the transition of $Flk1^+$ extraembryonic mesoderm towards endothelial and endothelial lineages, we used small molecule inhibitors to inhibit these two signaling pathways in an ES cell differentiation system modeling $Flk1^+$ extraembryonic mesoderm, in serum-free, feeder cell layer-free conditions. To obtain $Flk1^+PDGFR\alpha^-$ cells, we differentiated CCE mouse ES cells in serum-containing medium, on confluent OP9 feeder layers, for 4 days. The cells were then sorted by FACS and subsequently recultured in Collagen-IV-coated 6-well plates, in SFO3, a serum-free, chemically defined culture medium that was shown to support endothelial, and hematopoietic differentiation in a similar system.[109] The medium contained a combination hemopoietic factors: VEGF, EPO, IL-3 , G-CSF, and SCF, in the presence or absence of BMP signaling inhibitor LDN-193189 (called LDN thereafter), and/or canonical Wnt signaling inhibitor XAV939 (called XAV thereafter). "Wnt signaling" will thereafter mean only the canonical Wnt pathway, since the non-canonical ones are supposably

unaffected by XAV939. LDN inhibits BMP Type I receptors ALK-2, and ALK-3, preventing phosphorylation, and subsequent activation of Smad1/5/8, thus shutting down BMP signaling.[110] XAV inhibits TNKS, and thus stabilizes the Axin complex and inhibits Wnt-responsive gene activation.[111] After 4 days of culture, cells were harvested, and analyzed. (Fig. 7A-C)

After reculture on Collagen-IV, differences were visible by simple microscope observation: by day 2, the wells that contained the the BMP signaling inhibitor displayed hindered hematopoietic differentiation, and bigger, easier to see endothelial structures. At day 4 of differentiation, these differences could still be seen, although they were less obvious, probably because, by then, the cells looked a little less healthy. (Fig. 7D) The overall cell number that was retrieved from each duplicate was about the same in all conditions, although a statistically relevant 30% decrease was observed in the wells that contained both inhibitors. (Fig. 8) This probably reflects the reduced amount of hematopoietic cells that were retrieved from these wells, and not a in viability, and/or proliferation potential.

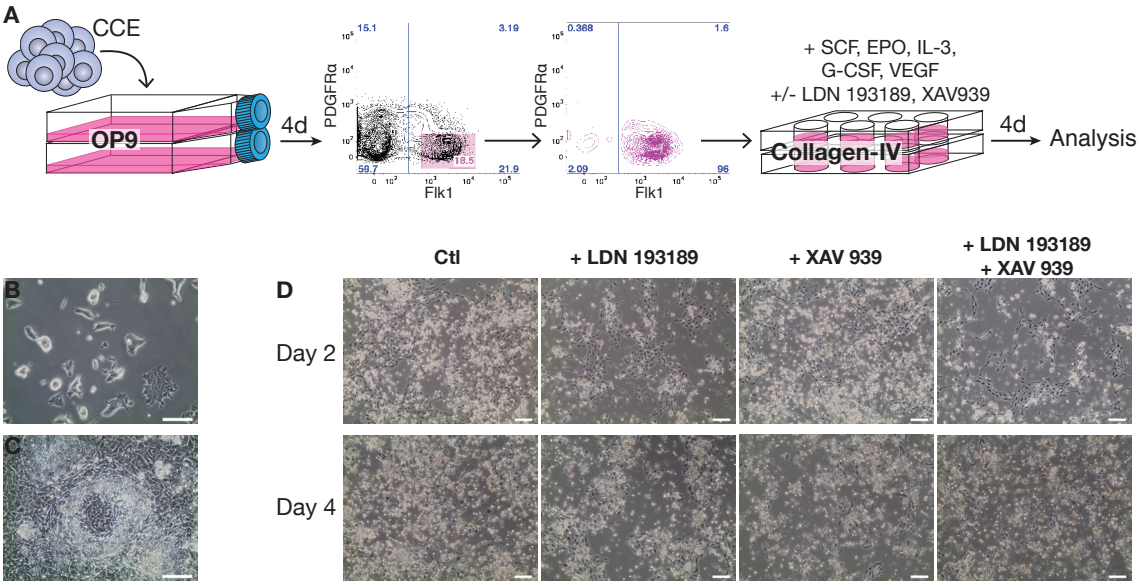

Figure 7. The differentiation system
A Model of the differentiation system used in this study. CCE cells were seeded on OP9 feeder layers, and differentiated for 4 days in serum-containing medium. Flk1^{+}PDGFRα^{-} cells were sorted and recultured in Collagen-IV-coated 6-well plates, in serum-free medium containing hemopoietic factors, in the presence or absence of LDN 193189 (400nM), and/or XAV939 (200nM). 4 days later, the cells were harvested and analyzed. **B** Colonies of undifferentiated CCE mouse ES cells before they were seeded. Phase contrast microscopy, 100x, scale bar = 100μm.. **C** Typical structure obtained after 4 days differentiation of CCE cells in serum-containing medium on OP9 feeder layer. Phase contrast microscopy, 100x, scale bar = 100μm. **D** Typical aspect of the cultures after 2, or 4 days of differentiation on Collagen-IV, using the differentiation system from **A**. Phase contrast microscopy, 50x, scale bar = 100μm.

We first wanted to observe how the fate of these cells was affected by the addition of the small molecule inhibitors. We thus checked the expression of endothelial and hematopoietic markers by flow cytometry analysis. The effect of the inhibitors was evident, and reproducible (n=6, or 7). BMP and Wnt signaling inhibition appears to work synergistically to restrict differentiation towards pre-HSC-like cells, defined by coexpression of VE-Cad and CD45: used separetly,

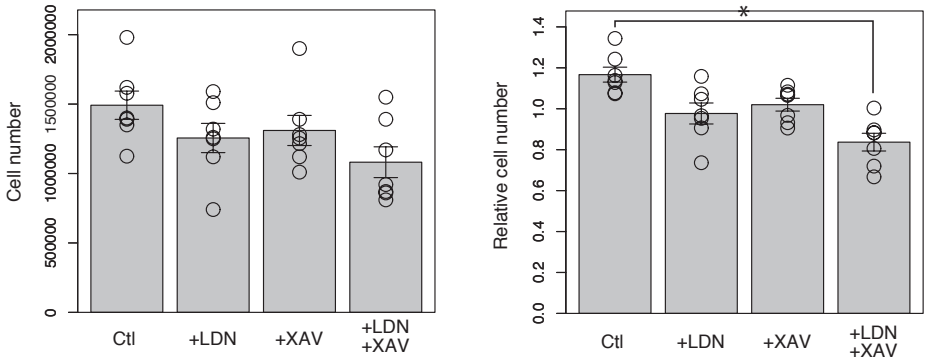

Figure 8. Cellularity is only slightly affected by LDN 193189 and XAV939
Number of cells retrieved per duplicate after reculture of Flk1+PDGFRα- on Collgen-IV for 4 days in serum-free medium containing hemopoietic factors, in the presence or absence of LDN 193189 (400nM), and/or XAV939 (200nM) The left bar plot shows the absolute cell count. The right bar plot represent cell number, normalized, for each experiment, to the mean of the experiment, to dampen starting cells proliferation potential-related variations. n=7, error bars: ±SEM, *: p-value<0.05/13

LDN and XAV had a similar effect; they lowered the number of these cells almost 2x. When both inhibitors were used together, the potential to give rise to VE-CAd^{+}CD45^{+} cells was lowered by about 4x. (Fig. 9A) A similar pattern, was observed for early hematopoietic cells (CD41^{+}CD45^{-}), further committed hematopoietic cells (CD41^{-}CD45^{+}), and macrophage progenitor cells (CD45^{+}CD11b^{+}): LDN and XAV deplete these cell pools by a factor 1.4, 1.9, and 1.7 respectively, and their effect appears to be cumulative, as these factors are approximately doubled when both small molecule inhibitors are used together: factor 2.3, 3.4, and 4.25, respectively. (Fig. 9E-F) This is consistent with the previous idea that BMP and Wnt signaling cooperate in the specification of hematopoietic fate. Hematopoietic progenitor cell (CD45^{+}c-Kit^{+}) number follows a slightly different pattern: although the depletion of this cell pool is higher when both BMP and Wnt signaling are inhibited, by a factor 2, LDN alone does not display any striking depleting effect, when XAV does (by a factor 1.45). (Fig. 9D) This data indicates that hematopoietic differentiation is restricted when BMP and Wnt signaling are suppressed. Suprisingly, the early hematopoietic progenitor cells pool (CD41^{+}c-Kit^{+}), however, is relatively unaffected by both inhibitors. (Fig. 9C)

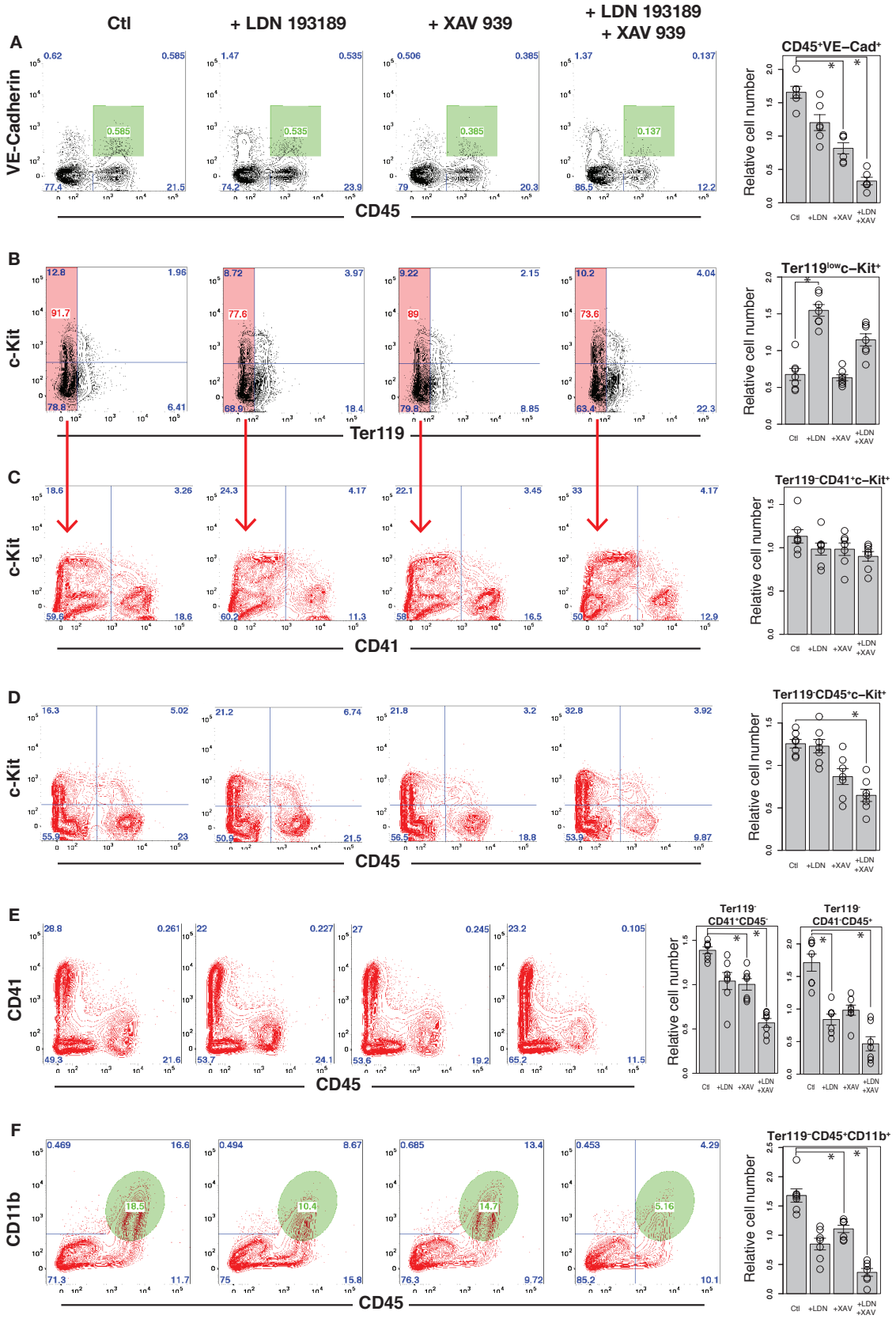

Figure 9. Inhibition of BMP and/or Wnt signaling alters the hematopoietic potential
Flow cytometry analysis of Flk1+PDGFRα- cells after 4 days of differentiation on Collagen-IV, in serum-free medium containing hemogenic factors. The red plots display only Ter119- cells. The bar plots on the right represent the percentage of cells expressing the indicated markers, multiplied by cell number, then normalized, for each experiment, to the mean of the experiment. n=7, error bars: ±SEM, *: p-value<0.05/13

LDN 193189 significantly expanded about 2x the proerythroblast pool, defined as Ter119^{low}c-Kit^{+}. Even though Wnt signaling was supposed to be required for the commitment to the primitive erythroid lineage,[59] XAV939 did not decrease the proerythroblast pool. However,

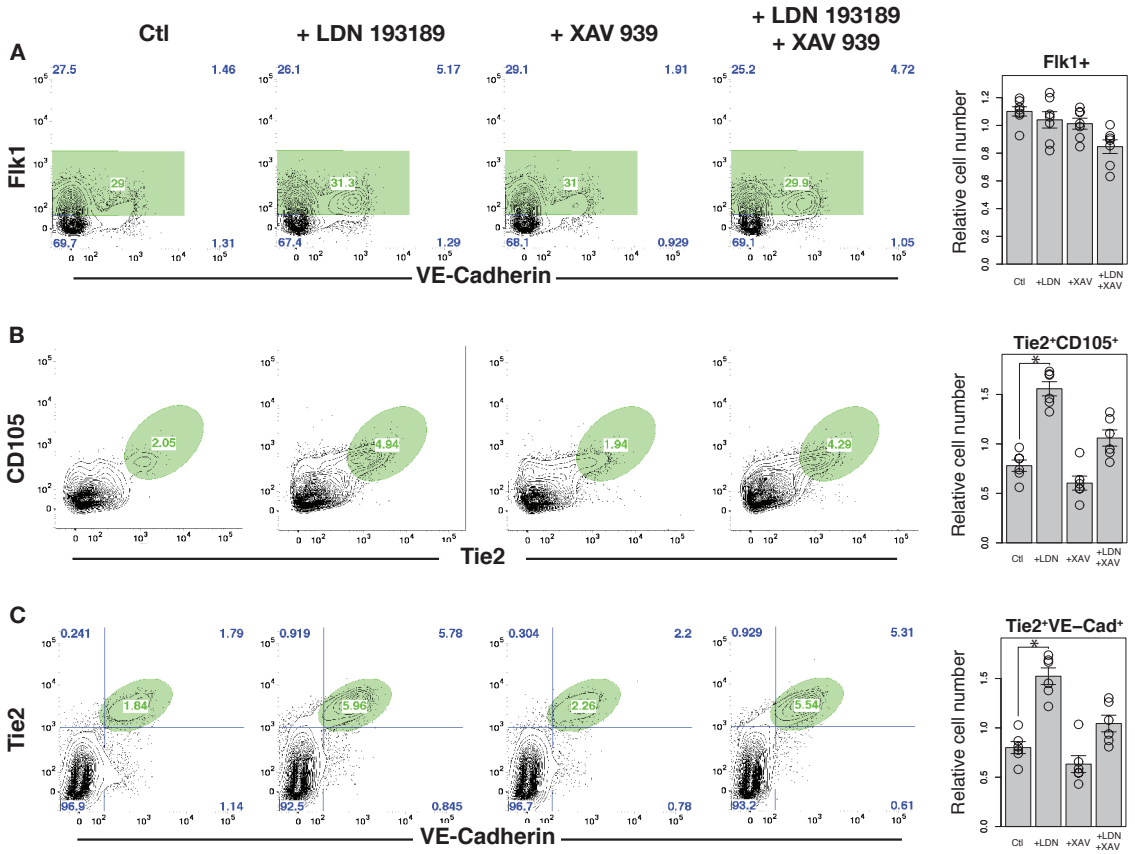

Figure 10. BMP signaling inhibition expands the endothelial compartment
Flow cytometry analysis of Flk1^{+}PDGFRα^{-} cells after 4 days of differentiation on collagen-IV, in serum-free medium containing hemogenic factors, in the presence or absence of LDN 193189 (400nM), and/or XAV939 (200nM). The bar plots on the right represent the percentage of cells expressing the indicated markers, multiplied by cell number, then normalized, for each experiment, to the mean of the experiment. Each experiment was done in duplicate, n=7, error bars: ±SEM, *: p-value<0.05/13

when both inhibitors were added together, the promoting effect of the BMP signaling inhibition seemed to be slightly dampened. (Fig. 9B) This erythroid cell pool was in our differentiation system the only hematopoietic compartment to be affected by BMP signaling in a manner that reproduces the observations made by the group of Todd Evans[84] with the Smad1 Tet-off system. This discrepancy might be the result of the different system that were used, as we performed this experiment on adherent cell cultures, when they used embryoid bodies. It could also be that Smad1 inhibition has a different effect than LDN-based suppression of the BMP signaling pathway.

Flk1 expressing cell number was virtually unaffected by LDN, XAV, or even a combination of both inhibitors. (Fig. 10A) Other endothelial cell pools ($CD105^+Tie2^+$, and $Tie2^+VE\text{-}Cad^+$),[112,113] on the other hand, were clearly expanded by a factor 2 when LDN was used alone, the effect of XAV used alone, and of both inhibitors toegether are less obvious, but seem consistent: reduction, and expansion, respectively, both by a factor 1.3. (Fig. 11B-C). The expansion of the endothelial compartment by LDN was quite a surprise, as *Gata2*, one of the genes driving endothelial differentiation is activated by BMP signaling.[117] The reason for that might be that, since hematopoietic differentiation is blocked, more cells keep an endothelial phenotype.

$Flk1^+PDGFR\alpha^-$ cells were also cultured on Collagen-I-coated glass culture slides, with the same serum-free medium and factors combination. The differentiation pattern was apparently identical to the one obtained with collagen-IV-coated well plates. In these cultures, similar effects of BMP and Wnt signaling on the differentiation towards the endothelial lineage were observed by immunostaining for Platelet endothelial cella adhesion molecule (PECAM-1, also known as CD31), and Intercellular cell adhesion molecule (ICAM2), two pan-endothelial markers.[114,115] In the wells containing LDN, the endothelial structures were clearly bigger. Furthermore, they looked to be the biggest when LDN was used alone. The flow cytometry data obtained for the endothelial lineage was thus confirmed by immunostaining. (Fig. 11)

To better understand the molecular mechanisms behind the effects of BMP and Wnt signaling inhibition on endothelial, and hematopoietic differentiation, we carried out qRT-PCR experiments. $Flk1^+PDGFR\alpha^-$ cells were harvested after 4 days reculture on Collagen-IV, and their total RNA was extracted. It was reverse-transcribed to cDNA, and qPCRs were performed. We targeted genes that are implicated in the transcriptional network that drives endothelial and hematopoietic differentiation program. Genes implicated in early events of this differentiation process, such as Runx1, Fli1, Scl, Lyl1, and Myb[116] expression followed a similar pattern: LDN, or XAV, alone did not significantly change the level of expression. When both inhibitors were added together, a small but remarkable increase in expression could be observed (1.26x, 1.21x, 1.58x, 1.41x, and 1.75x respectively). This pattern looks inversely proportional to the effect of the inhibitors on hematopoietic differentiation. Gata2, Lmo2, and Erg,[116] on the other hand are affected in a different manner by BMP and Wnt signaling inhibition. Gata2 was downregulated

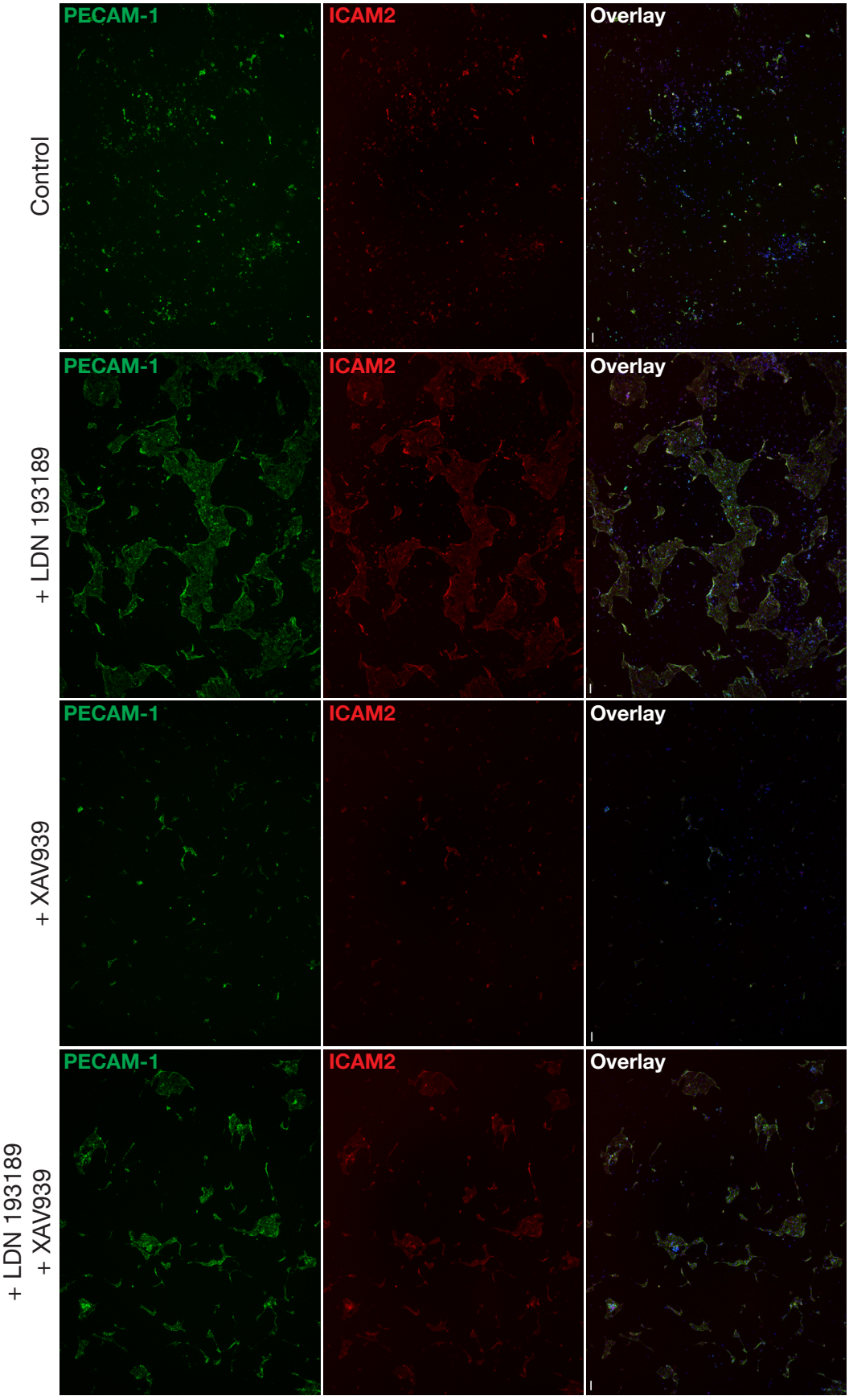

Figure 11. Endothelial structures are bigger in the LDN 193189-containing wells
Staining was done after the Flk1^{+}PDGFRα^{-} were recultured for 4 days on Collagen-IV. Green: PECAM-1, red: ICAM2. Fluorescence microscopy, 40x, scale bar: 100μm, n=2.

by LDN alone (0.67x), as expected since it is a direct target of BMP4.[117] Unexpectedly, if both inhibitors were added together, this downregulating effect of LDN on Gata2 expression was lost. However, XAV alone did not provoke any remarkable change in Gata2 expression. Lmo2 was unaffected by both inhibitors, which was rather surprising, as we expected it to follow a pattern similar to his interaction partners Scl and Lyl1.[116] Erg was significantly upregulated by BMP signaling expression (LDN only: 3.95x, LDN and XAV: 3.61x), but unaffected by Wnt signaling inhibition. This seems to reflect its importance in the endothelial differentiation process.[118] Suprisingly, the hematopoietic-specific transcription factor PU.1[119] was unaffected by both small molecule inhibitors. Gata1, on the other hand was clearly upregulated by both LDN and XAV (LDN only: 2.3x, XAV only: 5.6x, LDN + XAV: 3.6x). This increase in Gata1 expression is consistent with the expansion of the proerythroblast pool in the LDN-containing wells, as Gata1 is the key transcription factor of erythroid differentiation.[120] However, in the well where only Wnt signaling was inhibited, Gata1 upregulation is evident, but there was no increase in the erythroid cell pool. This tends to indicate that even though Gata1 is required to obtain erythroid cells, its expression level is not directly linked to the

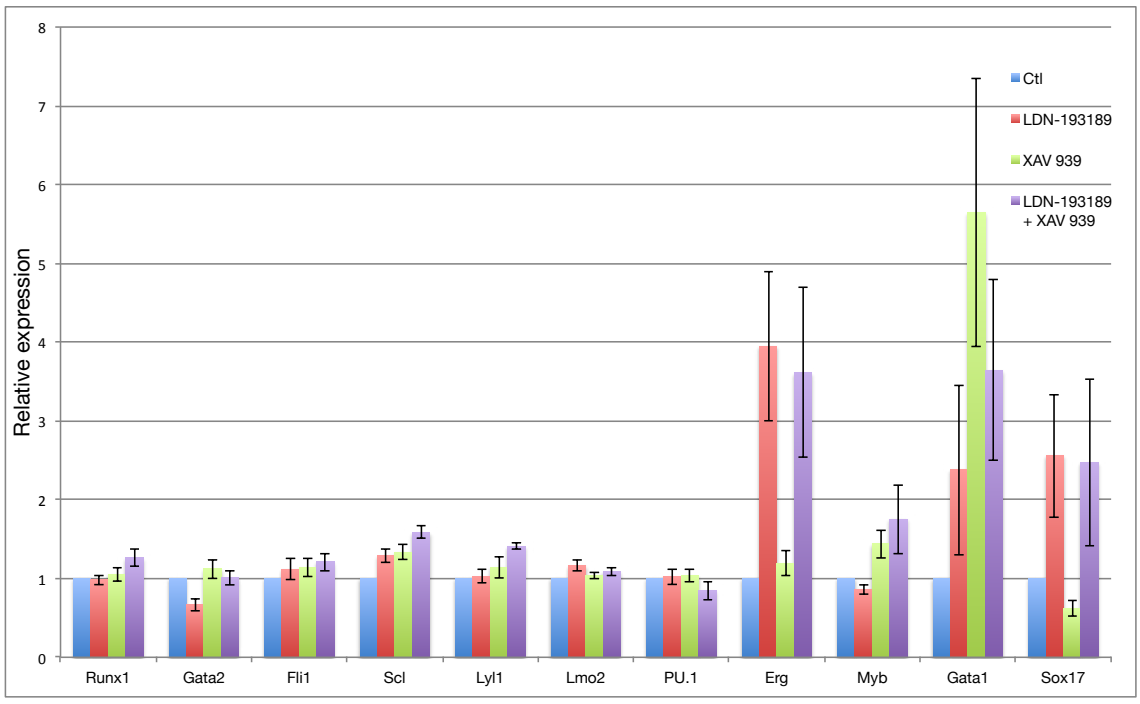

Figure 12. Differences in expression levels of key endothelial and hematopoietic trancription factors
Expression levels of key endothelial and hematopoietic transcription factors were assessed by qRT-PCR. Total RNA was extracted from Flk1+PDGFRα- cells recultured 4 days on Collagen-IV in serum-free medium containing hemopoietic factors, in the presence or absence of LDN 193189 (400nM), and/or XAV939 (200nM). Raw data was obtained using the Relative Standard Curve Method. It was then normalized using GAPDH as a reference. The bar plot represents fold changes relative to control. Each experiment was done in triplicate, n=4, error bars: ±SEM.

size of this cell pool. Finally, the definitive endothelial transcription factor Sox17 was as well upregulated only in the wells that contained LDN (LDN only: 2.56x, LDN + XAV: 2.48), which is consistent with the expansion of the endothelial cell pool in those wells. XAV only-continaing wells seem to have a slightly downregulated expression of Sox17 (0.62x). (Fig. 12)

The fact that the changes in gene expression are not as evident as the differences observed by flow cytometry analysis might be due to the fact that we performed the qRT-PCRs at day 4 of differentiation on Collagen-IV. The data might thus reflect more the result of the LDN and XAV signaling on the differentiation pattern than their effects on the transcription network itself. To obtain more information on that latter matter, we should perform again the same reactions, but after only 1 day of differentiation on collagen-IV, or in sorted populations after 4 days of differentiation. Furthermore, data analysis was made difficult for some of those genes, as their expression levels are very low, namely Erg, Myb, Gata1, and Sox17. This made the results quite variable, as indicated by the high standard error of the mean. (Fig. 12)

Expansion of a VE-Cad+CD45+ population in the yolk sac upon Etv2 overexpression in mouse embryo

Etv2 is one of the earliest markers of differentiation towards endothelial, and hematopoietic lineages in the mouse embryo. In zebrafish, its ortholog Etsrp is both necessary and sufficient to initiate vasculogenesis.[101] Etv2 is turned on before Flk1 expression, and it is expressed in the same region, the extraembryonic mesoderm. The *Etv2-/-* mutation is embryonically lethal.Embryos die around E9.5 from failure to develop blood, vessels, and endocardium.[46,100] Etv2 expression is very transient: as soon as the $Etv2^{+}$ cells commit to either endothelial, or hematopoietic fates, they lose its expression. To gain more insight on the spatial and temporal localization requisite expression pattern of Etv2, Dr. Hiroshi Kataoka developed a CAG promoter-controlled *Etv2-IRES-GFP* construct containing a floxed stop-cassette, and inserted it within the *ROSA26* locus. This mouse line could then be crossed with various Cre-recombinase (Cre) mouse line to allow the tissue-specific expression of the transgene.[121]

It was previsously shown by Dr. Kataoka that overexpressing Etv2 in the Vav,[122] and Sox17[123] compartments, that represent more definitive hematopoietic, and endothelial cells, respectively, does not affect embryonic development, and that these mice develop normally until adulthood

, although they seem to have a shorter life expectancy. (unpublished data) He also showed, however, that overexpressing Etv2 in the MesP1 compartment (early mesoderm),[124] is embryonically lethal. These embryos die around E11.5. They present a bleeding phenotype, and some abnormal structures in the yolk sac vasculature at this stage. (unpublished data) Continuing in the same direction Dr. Kataoka crossed *Tie2Cre*$^{WT/Tg}$ and *Rosa26-etv2-IRES-GFP*$^{Tg/Tg}$ mice in order to overexpress Etv2 in the whole endothelial compartment.[105] (Fig. 14A) He obtained data indicating that these embryos die also around E11.5 and that they are a phenocopy of the *Mesp1Cre*$^{WT/Tg}$*Rosa26-etv2-IRES-GFP*$^{Tg/WT}$ embryos. (unpublished data, Fig. 13)

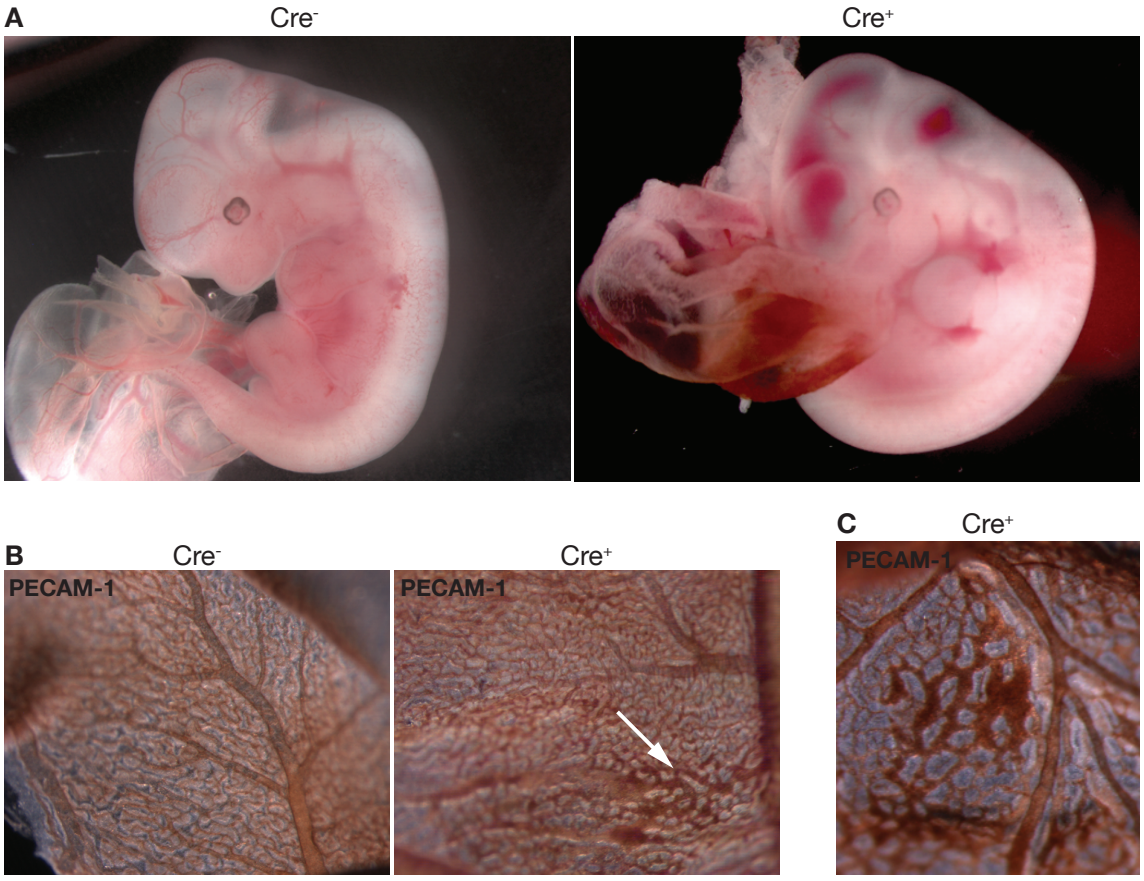

Figure 13. At E11.5, Tie2Cre$^{WT/Tg}$Rosa26-etv2-IRES-GFP$^{Tg/WT}$ embryos present a bleeding phenotype, and some abnormalities in the yolk sac vasculature
A E11.5 embryos, lateral view, the bleeding phenotype is evident in the Cre$^+$ embryo. **B** E11.5 yolk sacs. PECAM-1 immunohistochemistry staining. White arrow: abnormal vascular structure in the Cre$^+$ yolk sac. **C** Detail of an abnormal vascular structure in a E11.5 Cre$^+$ yolk sac. Cre$^-$: *Tie2Cre*$^{WT/WT}$*Rosa26-etv2-IRES-GFP*$^{Tg/WT}$ embryos, Cre$^+$: *Tie2Cre*$^{WT/Tg}$*Rosa26-etv2-IRES-GFP*$^{Tg/WT}$ embryos. Courtesy of Dr. Hiroshi Kataoka

We then further investigated on the mechanisms that allow Etv2 overexpression to lead to the death *in utero* of the *Tie2Cre*$^{WT/Tg}$*Rosa26-etv2-IRES-GFP*$^{Tg/WT}$ embryos (referred to Cre$^+$ embryos thereafter). We confirmed that the embryos are viable until E10.5, at which stage the proportion of live embryos is close to the Mendelian ratio : 38% for E9.5, and 49% for E10.5. This proportion

drops to 10% only for live born pups. (Table 2) The fact that we still obtain live pups that look normal (at least until 2 weeks after birth) indicates there is an escape mechanism that allow embryos to survive in spite of the transgene's presence. It is possible that the transgene-expressing cells are rapidly counter-selected during development: As Cre-recombination does not have a penetrance of 100%,[125] it is possible that the transgene-expressing cells are excluded from the endothelial, and/or hematopoietic compartment of the surviving embryos. This will have to be tested in the future as we didn't have enough time to perform this assay before the deadline for this report.

Stage	Total # of embryos	Cre-	Cre+	Cre+ with YS GFP pattern	Cre+/Total ratio
E9.5	29	18	11	4	0.38
E10.5	45	23	22	19	0.49
E14.5	5	2	3	0	0.6
P0	20	18	2	0	0.1

Table 1. Analysis of progeny of *Tie2Cre$^{WT/Tg}$* and *Rosa26-etv2-IRES-GFP$^{Tg/Tg}$* intercrosses

At E9.5, the Cre^{+} embryos did not display any gross vasculature defect, as assessed by Flk1 immunostaining. (Fig. 14B) The localization of the transgene-expressing cells in the Cre^{+} embryos was determined, taking advantage of the GFP reporter integrated in the construct. In the E10.5 embryo proper, these cells localized as expected in the vascular endothelium. (Fig. 14C) In the yolk sac, though, the Cre^{+} embryos displayed a clear typical pattern: the GFP+ cells formed small clusters, that recall the abnormal vascular structures found in the yolk sac of these embryos at E11.5. (Fig. 14D-E) This pattern of transgene expression was also observed in E9.5 yolk sacs (data not shown). However, it was not present on all E9.5 and E10.5 yolk sacs, and absent in all the E14.5 yolk sacs, (Table 2) further supporting the idea that there is a mechanism that allows some embryos to exclude transgene-expressing cells from the endothelial, and/or hematopoietic compartments in order to survive. The expression level of the transgene was not particularly high, which implies that the imaging probably does not show all the transgene-expressing cells.

In order to characterize the cell population that formed those clusters in the E10.5 yolk sacs of the Cre^{+} embryos, E10.5 embryo propers and yolk sacs were separated by dissection, dissociated into a single cell suspension, and analyzed by flow cytometry for their expression of several endothelial, and hematopoietic markers. Flow cytometry analysis also allowed us to assess with

more certainty which embryos were Cre$^+$, and which were Cre$^-$, when the diagnosis was uncertain, by checking for GFP expression. In the embryo proper, there was no change in the number of VE-Cad$^+$ cells, and surprisingly a 2-fold reduction in the number of CD45$^+$ and VE-Cad$^+$CD45$^+$ cells. (Fig. 15 & 16) In the yolk sac tissue, all three CD45$^+$, VE-Cad$^+$, and VE-Cad$^+$CD45$^+$ populations approximately doubled in cell number in the Cre$^+$ embryos (2.51x, 2.22x, and 2.7x, respectively). (Fig. 15 & 16) The fact that this VE-Cad, and CD45 double-positive cell pool was expanded more than 2 times in the Cre$^+$ embryos was very intriguing, as theses cells are

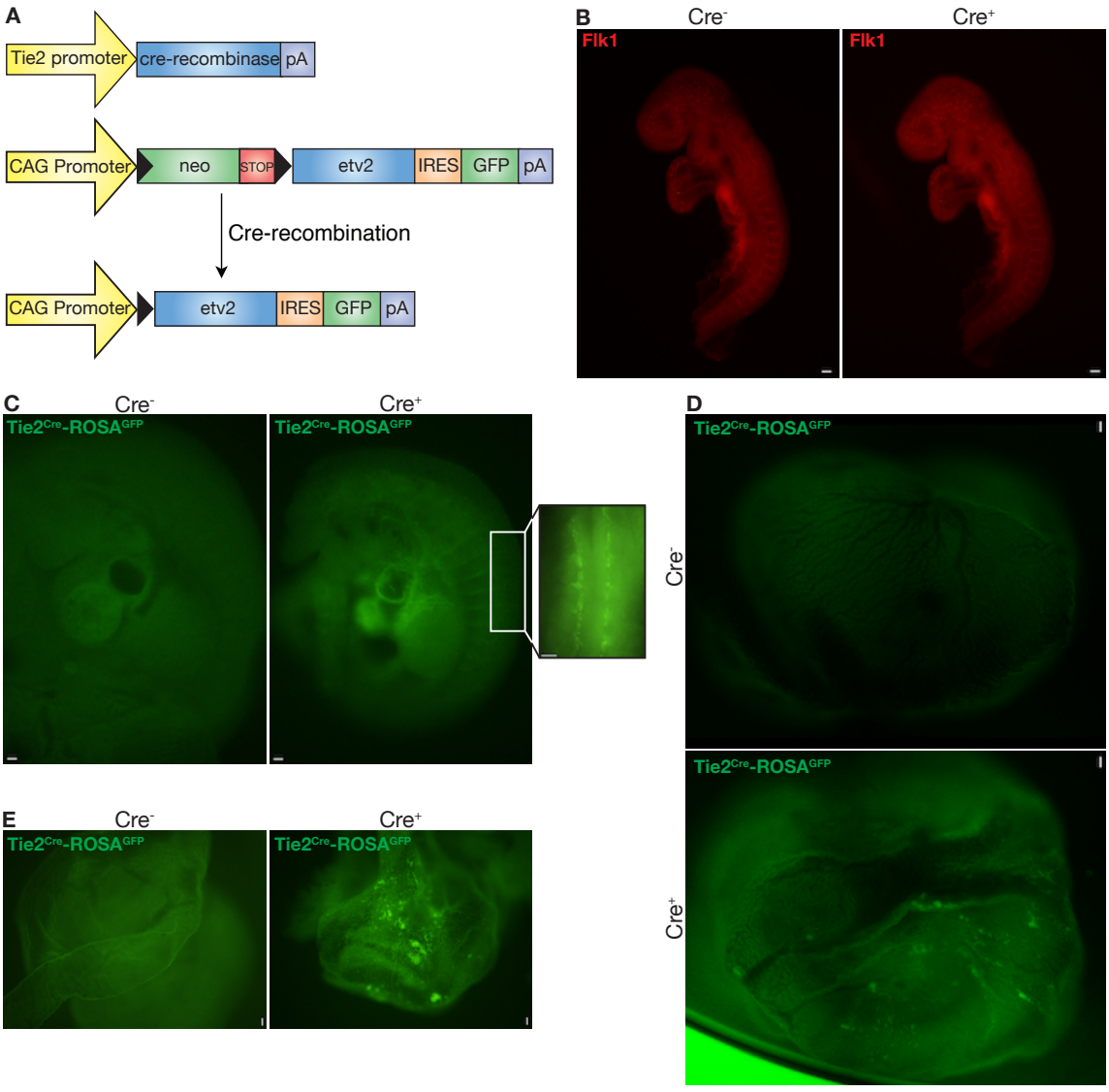

Figure 14. Transgene-expressing cells locate in the vasculature endothelium and form clusters on the yolk sac at E10.5
A The *Tie2Cre* construct, and the *Rosa26-etv2-IRES-GFP* construct, before and after Cre-recombination. **B** E9.5 vasculature (lateral view), immunostaining for Flk1. Fluorescence microscopy, 40x, scale bar=100μm. **C** Localization of the transgene-expressing cells in the E10.5 embryo proper (lateral view). Fluorescence microscopy, 40x, scale bar=100μm. Insert: transgene-expressing cells located in the intersomite vasculature (dorsal view). Fluorescence microscopy, 100x, scale bar=100μm. **D,E** Typical localization pattern, in clusters, of the transgene-expressing cells in E10.5 yolk sacs. Fluorescence microscopy, 40x, scale bar=100μm. Cre$^-$: *Tie2Cre$^{WT/WT}$Rosa26-etv2-IRES-GFP$^{Tg/WT}$* embryos, Cre$^+$: *Tie2Cre$^{WT/Tg}$Rosa26-etv2-IRES-GFP$^{Tg/WT}$* embryos.

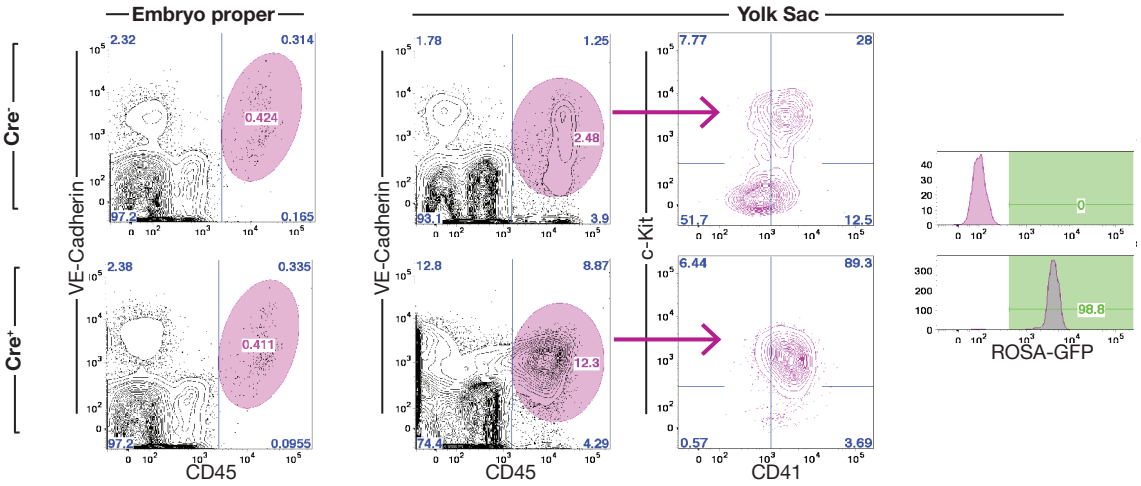

Figure 15. Expansion of a VE-Cad⁺CD45⁺ population in the E10.5 yolk sac of Cre⁺ embryos
Flow cytometry analysis plots from two representative experiments. Embryo propers and yolk sacs were separated by dissection, dissociated into single-cell suspensions, and analyzed separately. Cre⁻: *Tie2Cre*$^{WT/WT}$*Rosa26-etv2-IRES-GFP*$^{Tg/WT}$ embryos, Cre⁺: *Tie2Cre*$^{WT/Tg}$*Rosa26-etv2-IRES-GFP*$^{Tg/WT}$ embryos.

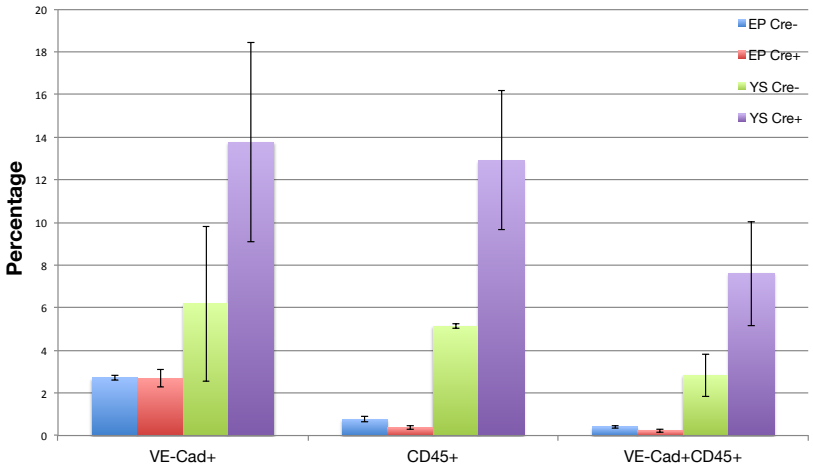

Figure 16. Summary of the flow cytometry analysis data from E10.5 embryo propers and yolk sacs
Flow cytometry analysis data. The gating that was used is showed in Fig. 15. Embryo propers and yolk sacs were separated by dissection, dissociated into single-cell suspensions, and analyzed separately. n=3, error bars: ±SEM. EP: embryo proper, YS: yolk sac, Cre⁻: Tie2Cre$^{WT/WT}$Rosa26-etv2-IRES-GFP$^{Tg/WT}$ embryos, Cre⁺: Tie2Cre$^{WT/Tg}$Rosa26-etv2-IRES-GFP$^{Tg/WT}$ embryos.

thought to represent pre-definitive-HSC-like cells. [66,126] Furthermore, we noticed that more than 90% of the VE-Cad⁺CD45⁺ found in the Cre⁺ embryos expressed the transgene. Most of them were also expressing c-Kit and CD41, when it was not the case for their counterparts in the Cre⁻ embryos,. (Fig. 15) There was thus an expansion of a population of immature hematopoietic cells upon overexpression of Etv2 in the E10.5 yolk sac in endothelial cells. These observations pushed to attempt to characterize better this VE-Cad⁺CD45⁺ population. We thus sorted these cells by FACS from E10.5 yolk sacs, and used them to perform a CFU

methylcellulose assay, a microarray analysis, and a B-cell assay. (Fig. 17) This was done aiming to determine the hematopoietic potential of these cells, and to obtain more insight on the downstream targets of Etv2. However, due to the small amount of time and the difficulty to obtain big numbers of these cells, these experiments were done only once, and need to be reproduced at least two more times to gain statistical significance.

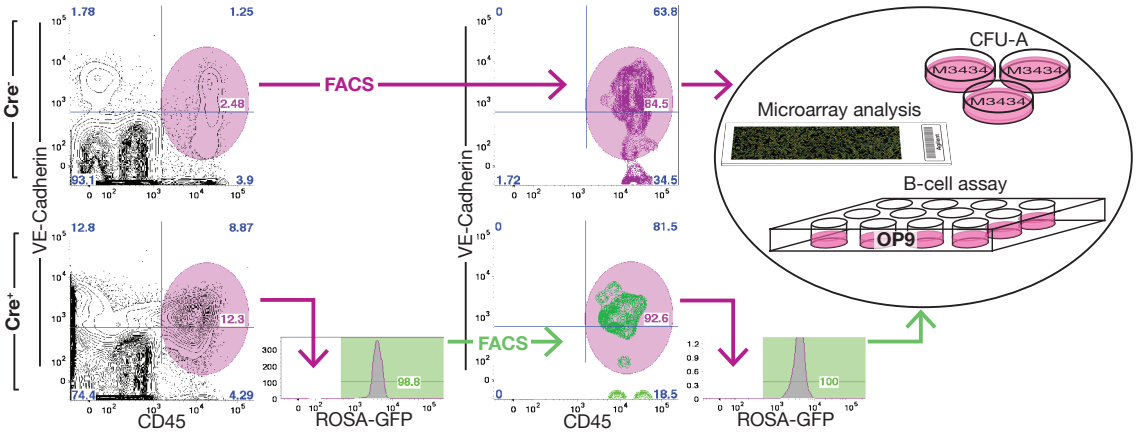

Figure 17. Sorting of VE-Cad⁺CD45⁺ cells from E10.5 yolk sacs and experimental plan
Ve-Cad⁺CD45⁺ cells from dissociated E10.5 yolk sacs were sorted following this plan. These cells were subsequently used for CFU-assay, microarray analysis, and B-cell assay. Cre⁻: *Tie2Cre$^{WT/WT}$Rosa26-etv2-IRES-GFP$^{Tg/WT}$* embryos, Cre⁺: *Tie2Cre$^{WT/Tg}$Rosa26-etv2-IRES-GFP$^{Tg/WT}$* embryos.

In the CFU-assay, 500 VE-Cad⁺CD45⁺ cells were seeded per dish, and colonies were counted 8 days later. In the dishes seeded with cells coming from Cre⁺ yolk sacs, all sorts of colony-forming units were observed: BFU-E, CFU-G, CFU-M, CFU-GM, and CFU-GEMM. (Fig. 18) We obtained an average of 61 colonies/500 cells seeded, which provides us with strong evidence that these cells have at least erythroid, and myeloid potential. For the Cre- control, as we were not able to obtain enough cells, from the Cre- yolk sacs, we had to sort the same population from wild type BL6 mice. In this control, in all three dishes of the triplicate, only 2 colonies were observed (2 CFU-GEMM). This latter result is hard to believe and is probably due to an unidentified technical problem. Unfortunately, there was no time to do this experiment one more time. Although the seeded cells were visible in the medium all along, they did not proliferate. The same cells generate large amounts of hematopoietic cells when seeded on an OP9 feeder layer for the B-cell assay.

The microarray analysis was performed using the new generation of arrays from Agilent, that allow the use of amounts of RNA as low as 10ng. Nevertheless, even in these conditions, it was

extremely difficult to obtain the 10'000 cells needed for each array, and we had to adapt our methodology according to this matter. In the end, two array experiments, with Cre$^+$ samples coming from 2 different litters were performed. For the Cre$^-$ control, however, VE-Cad$^+$CD45$^+$ cells coming from 3 different litters had to be combined to obtain enough RNA for a single microarray. Finally, the expression levels of the two Cre+ samples were average and compared to the single control. The statistical significance of these results is thus low, and we were unable to look for precedently uncharacterized potential targets of Etv2 in mouse.

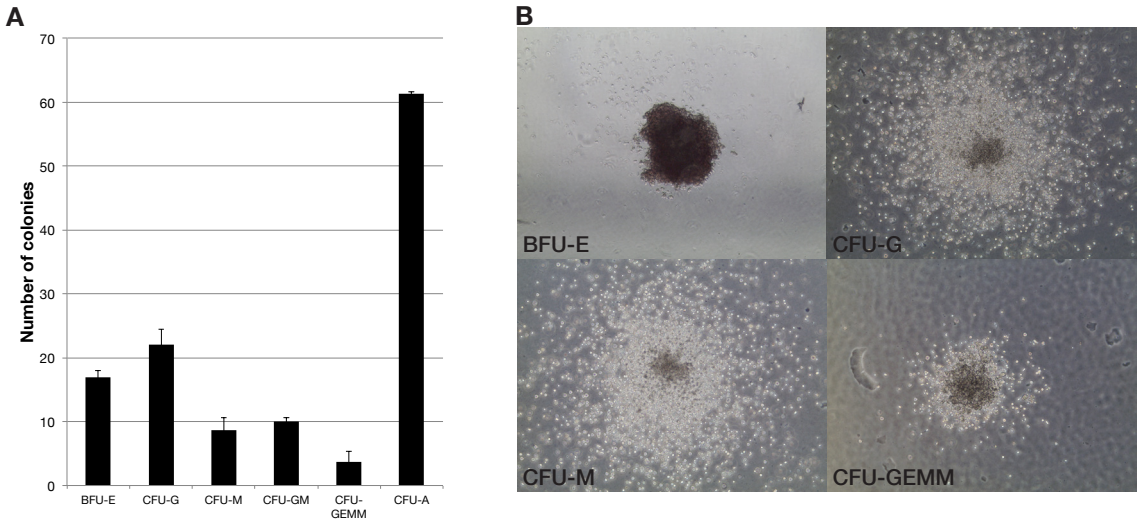

Figure 18. VE-Cad$^+$CD45$^+$ cells sorted from E10.5 Cre$^+$ yolk sacs have erythroid and myeloid potential
Sorted Ve-Cad$^+$CD45$^+$ cells from E10.5 Cre$^+$ yolk sacs were used to perform a CFU-assay. The assay was done in triplicate, 500 cells were seeded per dish, n=1. **A** Summary of the number of colonies per dish. **B** Typical aspect of BFU-E, CFU-G, CFU-M, and CFU-GEMM. Phase microscopy, 50x. Cre$^-$: *Tie2Cre$^{WT/WT}$Rosa26-etv2-IRES-GFP$^{Tg/WT}$* embryos, Cre$^+$: *Tie2Cre$^{WT/Tg}$Rosa26-etv2-IRES-GFP$^{Tg/WT}$* embryos.

Even though the experimental conditions were not optimal, the data accumulated from this experiment is rather sensible: a number of genes previously identified as being targets of Etv2 in similar experiments performed in zebrafish[127,128] were found to be upregulated in our system as well. Furthermore, there was a enrichment for endothelial-related genes in the most upregulated genes, and the major part of the key transcription factors linked to endothelial and hematopoietic differentiation were found to be at least slightly upregulated upon Etv2 overexpression.

The most 50 most upregulated are presented in Tables 3, amongst them, *Etv2* (13.95x) indicates that the transgene is working correctly. *VE-Cad* (11.4x), and *Flk1* (10.26x), two direct targets of Etv2,[127,128] provide some evidence that the experiment is at least accurate to some extent.

Fold change	Gene Symbol	Chromosome	Genbank Accession	Gene Name
52.16	Dysf	chr6	NM_001077694	dysferlin
33.83	C630004H02Rik	chr11	NM_175454	RIKEN cDNA C630004H02 gene
28.25	S100a8	chr3	NM_013650	S100 calcium binding protein A8 (calgranulin A)
24.91	Hapln1	chr13	NM_013500	hyaluronan and proteoglycan link protein 1
23.49	Dhrs2	chr14	NM_027790	dehydrogenase/reductase member 2
17.15	S100a9	chr3	NM_009114	S100 calcium binding protein A9 (calgranulin B)
17.12	Rgs3	chr4	NM_019492	regulator of G-protein signaling 3
16.79	Tspan18	chr2	NM_183180	tetraspanin 18
16.34	Ifi203	chr1	NM_001045481	interferon activated gene 203
15.54	Pde2a	chr7	NM_001143848	phosphodiesterase 2A, cGMP-stimulated
15.37	Fbp1	chr13	NM_019395	fructose bisphosphatase 1
15.31	Hopx	chr5	NM_175606	HOP homeobox
15.22	S100a16	chr3	NM_026416	S100 calcium binding protein A16
15.07	Ifi203	chr1	NM_001045481	interferon activated gene 203
14.66	**Slit2**	**chr5**	**NM_178804**	**slit homolog 2 (Drosophila)**
14.02	Mrgpra2b	chr7	NM_153101	MAS-related GPR, member A2B
14.01	Mrgpra6	chr7	NM_205821	MAS-related GPR, member A6
13.95	**Etv2**	**chr7**	**NM_007959**	**ets variant gene 2**
13.56	Mrgpra2a	chr7	NM_001172588	MAS-related GPR, member A2A
13.35	Csgalnact1	chr8	NM_172753	chondroitin sulfate N-acetylgalactosaminyltransferase 1
12.93	**Bcl6b**	**chr11**	**NM_007528**	**B-cell CLL/lymphoma 6, member B**
12.68	LOC677460	chr7	XM_001003789	similar to MAS-related GPR, member A4
12.54		chr1		lincRNA:chr1:175705225-175717250 reverse strand
11.89	**Notch4**	**chr17**	**NM_010929**	**Notch gene homolog 4 (Drosophila)**
11.57	Pnp2	chr14	NM_001123371	purine-nucleoside phosphorylase 2
11.56		chr6	XM_001472893	PREDICTED: Mus musculus hypothetical protein LOC100044678
11.40	**Cdh5/VE-Cad**	**chr8**	**NM_009868**	**cadherin 5**
11.31	Tdrd5	chr1	NM_001134741	tudor domain containing 5
11.05	Mmrn1	chr6	NM_027613	multimerin 1
11.04		chr2	XM_001478824	Putative uncharacterized protein Fragment
10.36		chr1		lincRNA:chr1:175705225-175717250 reverse strand
10.31	Crisp3	chr17	NM_009639	cysteine-rich secretory protein 3
10.26	**Kdr/Flk1**	**chr5**	**NM_010612**	**kinase insert domain protein receptor**
10.22	Fgr	chr4	NM_010208	Gardner-Rasheed feline sarcoma viral (Fgr) oncogene homolog
10.08	Clec1b	chr6	NM_019985	C-type lectin domain family 1, member b
10.02	Pglyrp1	chr7	NM_009402	peptidoglycan recognition protein 1
9.99	Myct1	chr10	NM_026793	myc target 1
9.94	2310065F04Rik	chr11	AK010044	RIKEN cDNA 2310065F04 gene
9.80	Cpa3	chr3	NM_007753	carboxypeptidase A3, mast cell
9.64	Serpina3g	chr12	NM_009251	serine (or cysteine) peptidase inhibitor, clade A, member 3G
9.60	Clec4e	chr6	NM_019948	C-type lectin domain family 4, member e
9.56	Galntl4	chr7	NM_173739	UDP-N-acetyl-alpha-D-galactosamine:polypeptide N-acetylgalactosaminyltransferase-like 4
9.51	**Il5ra**	**chr6**	**NM_008370**	**interleukin 5 receptor, alpha**
9.35	Tdrd5	chr1	NM_001134741	tudor domain containing 5
9.35	Tac4	chr11	NM_053093	tachykinin 4
9.26	Ptprb	chr10	NM_029928	protein tyrosine phosphatase, receptor type, B
9.21	Hopx	chr5	NM_175606	HOP homeobox
8.88	Clec1b	chr6	NM_019985	C-type lectin domain family 1, member b
8.81	Clec1b	chr6	NM_019985	C-type lectin domain family 1, member b

Table 3. Microarray analysis data: 50 most upregulated genes in VE-Cad$^+$CD45$^+$ cells sorted from E10.5 Cre$^+$ yolk sacs
Relative expression, compared to Cre$^-$ control. Bold: endothelial-, or hematopoietic-related genes. Cre$^-$: *Tie2Cre$^{WT/WT}$Rosa26-etv2-IRES-GFP$^{Tg/WT}$* embryos, Cre$^+$: *Tie2Cre$^{WT/Tg}$Rosa26-etv2-IRES-GFP$^{Tg/WT}$* embryos.

In this list of 50 genes, we found as well the endothelial-related gene *Slit2* (14.66), and the hematopoiesis-related genes BCL6b (12.93x), Notch4 (11.89x), and IL5Ra (9.51x). *ESAM*, that was identified as a target of Etsrp,[128] was also upregulated in our system (7.66x). The same thing was true for Ldb2 (8.794x), Hapln1 (24.91x), BMP2 (5.11x),[127] and Tie2 (5.69x).[66]

The 50 most downregulated genes are presented in Table 4. Etv2 has been described as an activator. Nevertheless we identified a quantity of downregulated genes. These hits could simply be indirect targets, Etv2 could have a different mechanism of action than Etsrp, they could

Fold change	Gene Symbol	Chromosome	Genbank Accession	Gene Name
-39.82	**Cfh**	**chr1**	**NM_009888**	**complement component factor h**
-37.43	**Emr1**	**chr17**	**NM_010130**	**EGF-like module containing, mucin-like, hormone receptor-like sequence 1**
-36.14	AI607873	chr1	XM_001479984	expressed sequence AI607873
-33.58		chr1		lincRNA:chr1:175653557-175671940 reverse strand
-32.68	Clec4a1	chr6	NM_199311	C-type lectin domain family 4, member a1
-32.26		chr1		lincRNA:chr1:175653557-175671940 reverse strand
-30.78	**Emr1**	**chr17**	**NM_010130**	**EGF-like module containing, mucin-like, hormone receptor-like sequence 1**
-29.45	Trem2	chr17	NM_031254	triggering receptor expressed on myeloid cells 2
-28.24	Timp2	chr11	NM_011594	tissue inhibitor of metalloproteinase 2
-26.99	Lpl	chr8	NM_008509	lipoprotein lipase
-26.16	**Col1a1**	**chr11**	**NM_007742**	**collagen, type I, alpha 1**
-25.43	**C1qb**	**chr4**	**NM_009777**	**complement component 1, q subcomponent, beta polypeptide**
-25.19	Ccl7	chr11	NM_013654	chemokine (C-C motif) ligand 7
-24.19	Itgb5	chr16	NM_010580	integrin beta 5
-24.11	Slc40a1	chr1	NM_016917	solute carrier family 40 (iron-regulated transporter), member 1
-23.76	5430435G22Rik	chr1	NM_145509	RIKEN cDNA 5430435G22 gene
-23.61	Tgfbi	chr13	NM_009369	transforming growth factor, beta induced
-23.46	**Cd83**	**chr13**	**NM_009856**	**CD83 antigen**
-23.30		chr1		lincRNA:chr1:175653557-175671940 reverse strand
-22.74	Lpl	chr8	NM_008509	lipoprotein lipase
-22.19		chr1		lincRNA:chr1:175654606-175672031 reverse strand
-21.89	Atf3	chr1	NM_007498	activating transcription factor 3
-21.48	Slc15a3	chr19	NM_023044	solute carrier family 15, member 3
-20.60	Ahnak	chr19	NM_009643	AHNAK nucleoprotein (desmoyokin)
-20.43	**C1qa**	**chr4**	**NM_007572**	**complement component 1, q subcomponent, alpha polypeptide**
-20.13	**C1qc**	**chr4**	**NM_007574**	**complement component 1, q subcomponent, C chain**
-19.94	Mrc1	chr2	NM_008625	mannose receptor, C type 1
-19.86	Gas6	chr8	NM_019521	growth arrest specific 6
-19.82	**Ly86**	**chr13**	**NM_010745**	**lymphocyte antigen 86**
-19.65	Nupr1	chr7	NM_019738	nuclear protein 1
-19.49	**Fcgrt**	**chr7**	**NM_010189**	**Fc receptor, IgG, alpha chain transporter**
-19.42	P2ry6	chr7	NM_183168	pyrimidinergic receptor P2Y, G-protein coupled, 6
-18.41	Dab2	chr15	NM_023118	disabled homolog 2 (Drosophila)
-18.37	Pdlim4	chr11	NM_019417	PDZ and LIM domain 4
-18.01	Aif1	chr17	NM_019467	allograft inflammatory factor 1
-17.93	Ccl2	chr11	NM_011333	chemokine (C-C motif) ligand 2
-17.44	Gap43	chr16	NM_008083	growth associated protein 43
-17.32	Ctss	chr3	NM_021281	cathepsin S
-16.96	Ccl12	chr11	NM_011331	chemokine (C-C motif) ligand 12
-16.77	Batf3	chr1	NM_030060	basic leucine zipper transcription factor, ATF-like 3
-15.88	Ckb	chr12	NM_021273	creatine kinase, brain
-15.69	Pld4	chr12	NM_178911	phospholipase D family, member 4
-15.10	Lrp1	chr10	NM_008512	low density lipoprotein receptor-related protein 1
-14.97	Tmem51	chr4	NM_145402	transmembrane protein 51
-14.96	LOC100048875	chr9	XM_001472585	similar to chemokine receptor CX3CR1
-14.79	Mcoln2	chr3	NM_026656	mucolipin 2
-14.07	Ms4a6c	chr19	NM_028595	membrane-spanning 4-domains, subfamily A, member 6C
-14.05	Slco2b1	chr7	NM_175316	solute carrier organic anion transporter family, member 2b1
-14.02	**Col1a2**	**chr6**	**NM_007743**	**collagen, type I, alpha 2**
-13.83	Fcrls	chr3	NM_030707	Fc receptor-like S, scavenger receptor
-13.78	Cx3cr1	chr9	NM_009987	chemokine (C-X3-C) receptor 1

Table 4. Microarray analysis data: 50 most downregulated genes in VE-Cad^{+}CD45^{+} cells sorted from E10.5 Cre^{+} yolk sacs
Relative expression, compared to Cre^{-} control. Bold: mesenchymal-, or hematopoietic-related genes. Cre^{-}: *Tie2Cre$^{WT/WT}$Rosa26-etv2-IRES-GFP$^{Tg/WT}$* embryos, Cre^{+}: *Tie2Cre$^{WT/Tg}$Rosa26-etv2-IRES-GFP$^{Tg/WT}$* embryos.

represent false hits, or Etv2 could have also a silencer activity. Amongst these genes, we identified many hits related to macrophage function, such as complement components: *Cfh* (-39.82x), *C1qb* (-25.42x), *C1qa*(-20.44x), and *C1qc* (-20.12x), and *Fcgrt* (-19.49x). Which suggests that the cells coming from Cre+ yolk sac are indeed more immature in their hematopoietic phenotype than their Cre^{-} counterparts. Mesenchymal collagen genes were also found to be enriched in the list of the downregulated genes: *Col1a1* (-26.12x), and *Col1a2* (-14.02x).

Fold change	Gene Symbol	Chromosome	Genbank Accession	Gene Name
8.30	Tjp1	chr7	NM_009386	tight junction protein 1
8.18	Nrarp	chr2	NM_025980	Notch-regulated ankyrin repeat protein
7.66	Esam	chr9	NM_027102	endothelial cell-specific adhesion molecule
7.65	Rasip1	chr7	NM_028544	Ras interacting protein 1
7.04	Klrb1c	chr6	NM_001159904	killer cell lectin-like receptor subfamily B member 1C
6.51	Vegfc	chr8	NM_009506	vascular endothelial growth factor C
6.48	Tgfbr3	chr5	NM_011578	transforming growth factor, beta receptor III
6.42	Bmp8a	chr4	NM_007558	bone morphogenetic protein 8a
6.15	Zfpm2	chr15	NM_011766	zinc finger protein, multitype 2
6.12	Ecscr	chr18	NM_001033141	endothelial cell-specific chemotaxis regulator
5.75	Cd93/AA4.1	chr2	NM_010740	CD93 antigen
5.73	Gimap4	chr6	NM_174990	GTPase, IMAP family member 4
5.69	Tek/Tie2	chr4	NM_013690	endothelial-specific receptor tyrosine kinase
5.19	Robo4	chr9	NM_028783	roundabout homolog 4 (Drosophila)
5.11	Bmp2	chr2	NM_007553	bone morphogenetic protein 2
-5.13	C5ar1	chr7	NM_001173550	complement component 5a receptor 1
-5.19	Cd86	chr16	NM_019388	CD86 antigen
-5.47	Bcl2a1d	chr9	NM_007536	B-cell leukemia/lymphoma 2 related protein A1d
-5.74	Lifr	chr15	NM_013584	leukemia inhibitory factor receptor
-6.14	Bmpr1a	chr14	NM_009758	bone morphogenetic protein receptor, type 1A
-6.18	Cd14	chr18	NM_009841	CD14 antigen
-6.48	Tlr2	chr3	NM_011905	toll-like receptor 2
-7.05	Msr1	chr8	NM_031195	macrophage scavenger receptor 1
-7.24	Cd33	chr7	NM_001111058	CD33 antigen
-7.36	Cd68	chr11	NM_009853	CD68 antigen
-7.49	Bcl2a1c	chr9	NM_007535	B-cell leukemia/lymphoma 2 related protein A1c
-7.52	Csf1r	chr18	NM_001037859	colony stimulating factor 1 receptor
-7.68	Blnk	chr19	NM_008528	B-cell linker
-7.71	Cfp	chrX	NM_008823	complement factor properdin
-7.90	Tlr13	chrX	NM_205820	toll-like receptor 13
-8.01	Cfb	chr17	NM_008198	complement factor B
-8.62	Hck	chr2	NM_001172117	hemopoietic cell kinase
-9.20		chr12	AK088666	immunoglobulin heavy chain 6 (heavy chain of IgM) Gene
-10.32	Tlr1	chr5	NM_030682	toll-like receptor 1
-11.45	Etv5	chr16	NM_023794	ets variant gene 5
-12.45	C3ar1	chr6	NM_009779	complement component 3a receptor 1
-13.08	Col3a1	chr1	NM_009930	collagen, type III, alpha 1
-13.22	Fcgr1	chr3	NM_010186	Fc receptor, IgG, high affinity I

Table 5. Microarray analysis data: other endothelial-, hematopoietic-, or mesenchymal-related genes differentially expressed in VE-Cad$^+$CD45$^+$ cells sorted from E10.5 Cre$^+$ yolk sacs
Remaining endothelial-, hematopoietic-, or mesenchymal-related genes that display a fold change in expression >5. Relative expression, compared to Cre$^-$ control. Cre$^-$: *Tie2Cre$^{WT/WT}$Rosa26-etv2-IRES-GFP$^{Tg/WT}$* embryos, Cre$^+$: *Tie2Cre$^{WT/Tg}$Rosa26-etv2-IRES-GFP$^{Tg/WT}$* embryos.

Fold change	Gene Symbol	Chromosome	Genbank Accession	Gene Name
4.03	Gata2	chr6	NM_008090	GATA binding protein 2
3.67	Erg	chr16	NM_133659	avian erythroblastosis virus E-26 (v-ets) oncogene related
3.16	Gfi1b	chr2	NM_008114	growth factor independent 1B
2.76	Eng/CD105	chr2	NM_001146350	endoglin
2.60	Meis1	chr11	NM_010789	Meis homeobox 1
2.16	Myb	chr10	NM_010848	myeloblastosis oncogene
2.01	Lmo2	chr2	NM_008505	LIM domain only 2
1.66	Kit	chr5	NM_001122733	kit oncogene
1.60	Fli1	chr9	NM_008026	Friend leukemia integration 1
1.54	Tal1/Scl	chr4	NM_011527	T-cell acute lymphocytic leukemia 1
1.25	Runx1	chr16	NM_009821	runt related transcription factor 1
1.23	Lyl1	chr8	NM_008535	lymphoblastomic leukemia 1
1.12	Icam2	chr11	NM_010494	intercellular adhesion molecule 2
-1.11	Gata1	chrX	NM_008089	GATA binding protein 1
-1.35	Bmp4	chr14	NM_007554	bone morphogenetic protein 4

Table 6. Microarray analysis data: expression levels of other endothelial/hematopoietic major transcription factors in VE-Cad$^+$CD45$^+$ cells sorted from E10.5 Cre$^+$ yolk sacs
Other endothelial/hematopoietic major transcription factors that display a fold change in expression <5. Relative expression, compared to Cre$^-$ control. Cre$^-$: *Tie2Cre$^{WT/WT}$Rosa26-etv2-IRES-GFP$^{Tg/WT}$* embryos, Cre$^+$: *Tie2Cre$^{WT/Tg}$Rosa26-etv2-IRES-GFP$^{Tg/WT}$* embryos.

Table 5 presents the rest of the genes that have been precedently associated to endothelial, hematopoietic, mesenchymal differentiation, and that are differentially expressed by at least a 5-fold change. Table 6 lists the major endothelial/hematopoietic transcription factors. We observed that Gata2, Erg, Gfi1b, Meis1, Myb, and Lmo2[116] see their expression level increase at least 2x upon Etv2 overexpression. Which is consistent with what was shown in the two zebrafish experiments. Obviously, all the hits presented here will have to be verified by repeating this experiment a few more times, but this preliminary data seems fairly consistent with what can be found in the literature, and with what was shown by the other experiments.

We also prepared a B-cell assay, in which sorted VE-Cad$^+$CD45$^+$ cells were recultured for 14days, in serum-containing medium supplemented with SCF, Flt3L, and IL-7, on OP9 feeder layer. At the time of writing, the B-cell assay was still underway (day 12), and the data will thus be only presented in the oral defense of the project. From the look of the cultures, it would seem that both Cre$^+$ and Cre- cells are proliferating, and that this proliferation is significantly more extensive in the Cre$^-$ control cells-containing wells.

5. Discussion

Effects of BMP and Wnt signaling inhibition on the differentiation of a Flk1$^+$ extraembryonic mesoderm in vitro model

Using an *in vitro* differentiation system that mimics Flk1$^+$ extraembryonic mesoderm, we were able to provide evidence that, after that stage, BMP and Wnt signaling still play a big role in the differentiation towards endothelial, and hematopoietic lineages. What is more, these effects appear to be cumulative, indicating these two pathways act cooperatively, as it was previously suggested.[79] Moreover, our results seem to be consistent with similar experiments that have been done by an other group.[81]

BMP signaling suppression leaded to an expansion of the endothelial, and erythroid compartments, and in a restriction of the hematopoietic cell pool. An explanation for this could be that BMP signaling inhibition prevents commitment towards hematopoietic lineage. Thus, the endothelial cell compartment could be expanded through either the inability of Flk1$^+$ extraembryonic mesoderm cells to become angioblasts, or the incapacity of hemogenic

endothelial cells to commit to a hematopoietic fate, or a combination of both. This promotion of the definitive endothelial fate by BMP signaling inhibition was further supported by the higher expression level of Sox17.[123] We thus speculate that this effect might be mediated by inactivation of Runx1: interaction between BMP signaling and Runx1 has already been suggested in the literature.[129] Moreover, *in vivo*, Runx1-expressing regions often overlap with BMP4 expression.[78] In addition, *Runx1*$^{-/-}$ mice have been shown to keep erythroid differentiation, but to lack other hematopoietic cell types, a phenotype close to what we observed in our culture system.[70] In the future, a closer look at the erythroid cells that were obtained in the LDN-containing wells could be very informative on this matter, as these cells have been shown to be abnormal in the *Runx1*$^{-/-}$ mice.[62]

Wnt signaling inhibition, on the other hand, appears to affect definitive hematopoiesis, but we did not observe an expansion of the erythroid and endothelial cell pools. This suggests that the mechanism of action is different. This idea is supported by the fact that Wnt and BMP signaling inhibition appear to act synergistically to suppress definitive hematopoiesis. Wnt signaling has been suggested to activate the Notch signaling pathway, which is a key factor in the transition towards definitive hematopoietic fate.[67,130] There is thus a possibility that Wnt signaling suppression leads to reduced Notch activation, and thus to restricted transition from hemogenic endothelial cells to the definitive hematopoietic lineage. This hypothesis could be assessed by testing if inhibition of the Notch signaling pathway leads to a similar phenotype in the same culture system.

In the future, if our hypothesis turn out to be correct, they will have to be tested in vivo. We can thus imagine creating conditional knockout mice that lose ALK-2 and ALK-3, or TNKS-1 and TNKS-2 expression at a precise time point, using either a Tet-off system and doxicycline injections, or a Cre-Lox system that excises these genes upon Flk1 expression, using a Flk1^{Cre} construct.

Expansion of a VE-Cad+CD45+ population in the yolk sac upon Etv2 overexpression in mouse embryo

In this part of the project, we used a Cre conditional knock-in system that allowed the overexpression of Etv2 in the Tie2 compartment. It permitted us to gain more insight in the

mechanisms of action of what we think is the master gene of endothelial , and hematopoietic development in the mouse embryo.

We were able to show that overexpressing Etv2 in the early endothelial compartment is embryonically lethal: the embryos die *in utero* around E11.5, presenting a bleeding phenotype, and some abnormal structures in the yolk sac vasculature. At day E9.5 and E10.5, the yolk sac of the Cre^+ embryos presented a typical pattern consisting in clusters of transgene-expressing cells. With flow cytometry analysis, we noticed the expansion of a VE-Cad^+CD45^+ cell population in the yolk sac of E10.5 Cre^+ embryos. The vast majority of these cells expressed the transgene, as well as c-Kit and CD41, contrarily to the same population isolated from Cre^- embryos. We thus suggested that the transgene-expressing cells represent a more immature hematopoietic population than their control, transgene-negative counterparts.

We then tried to further characterized this Etv2-overexpressing cell population, and found out that they have extensive erythroid and myeloid potential. Also, they seemed to express higher levels of numerous endothelial-related genes, and lower expression of mesenchymal-, and macrophage-related genes, as assessed by microarray analysis. Many of the major endothelial/ hematopoietic transcription factors were upregulated as well, although to a lesser extent.

One possible explanation for the phenotype observed in our system is illustrated by Figure 19. We think that hemogenic endothelial cells need to completely lose Etv2 expression in order to differentiate into definitive endothelial cells. Etv2 overexpression in those cells thus keeps them from doing so. This probably results in an accumulation of immature hemogenic endothelial cells. The data we obtained with the CFU-assay and from the look of the cells in the B-cell assay after 12 days of reculture indicate that hematopoietic differentiation is not much affected by the overexpression of Etv2. Thus, since there is an expanded pool of hemogenic endothelial cells, the pre-definitive-HSC number is also increased, which is reflected by the expansion of the VE-Cad^+CD45^+ cell population in the E10.5 yolk sac. This hypothesis will need to be further tested: the cells obtained in the CFU-assay will have to be more carefully observed, to see if they are fully normal, especially in their marker gene expression signature (especially VE-Cad and c-Kit). The B-cell assay will give us more information on the defninitive hematopoietic stem cell potential of

the Etv2-overexpressing cells. The endothelial potential of these cells will also have to be tested, probably by culturing them in the presence of VEGF, and checking for the formation of vascular-like structures.

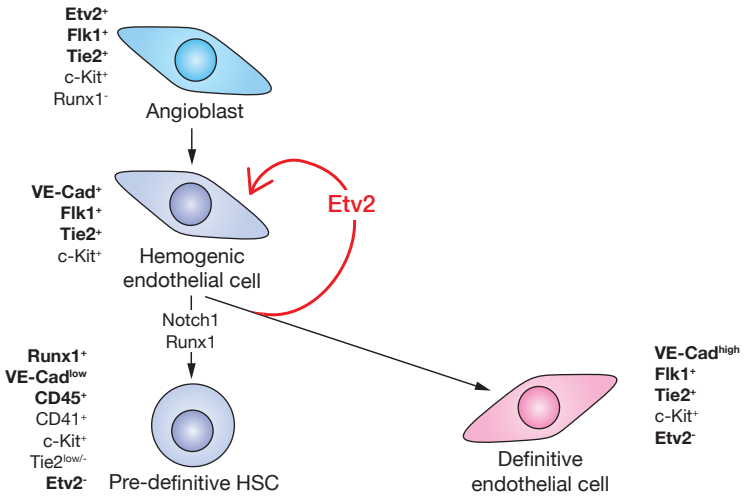

Figure 19. One possible explanation for the observed phenotype in the *Tie2Cre$^{WT/Tg}$Rosa26-etv2-IRES-GFP$^{Tg/WT}$* embryos
Etv2 overexpression keeps the hemogenic endothelial cells from differentiate further towards the endothelial lineage (red arrow). These cells stay thus in a more immature state. Hematopoietic differentiation, on the other hand, is not affected by Etv2 overexpression.

The data that we accumulated with these experiments, combined with the finding that overexpression of Etv2 in the Sox17 and Vav compartment is not lethal, strongly suggests that Etv2 needs the cells in which it is expressed to be somehow primed to be responsive to it. It appears that the cells that already have downregulated Etv2 during their differentiation will not revert back to a state that is affected by its overexpression. Also, we were able to obtain a good indication on the developmental window in which Etv2 downregulation is essential for the viability of the embryo: the cells that seem to be most affected by its overexpression are probably located in the yolk sac, and appear to be very similar to the ones we defined as hemogenic endothelial cells.

Kôbe, June 24th 2011

Matteo Pluchinotta

6. Acknowledgments

I would like to thank from the bottom of my heart Nishikawa-sensei, Kataoka-sensei, Satomi-sensei, and Hayashi-san for their immensely precious help and endless patience. I apologize for all the time that you lost because of me, I have learned so much from you! ありがとうございます! Thank you to Professor Yann Barradon, and to the EPFL exchange program staff, that made all of this possible. I thank as well the Swiss-Japan Association for Engineers and Scientists, for their generous financial support. I would also like to thank Tanaka-san, Kobayashi-san, Martin, Julien, Igor, and Moriwaki-san for their advices, Matsuo-san for the 神戸ビーフ and the ラーメン tour, and everybody else in the Laboratory for Stem Cell Biology, and in RIKEN CDB for their warm welcome. I thank as well Ryoko "人ごさま", Minamino-san, and the PLUS.S family for the good times spent together. Thank you to my family for their comprehension, and moral and financial support, and thank you to my friends for their presence. Finally, thank you to Japan, and more specifically Kôbe, for being such a nice place to spend a year in, and thank you to all the mice that bravely gave their life on the altar of my master's project.

7. Bibliography

1. Evans, M.J. & Kaufman, M.H. Establishment in culture of pluripotential cells from mouse embryos. Nature 292, 154-156(1981).
2. Martin, G.R. Isolation of a pluripotent cell line from early mouse embryos cultured in medium conditioned by teratocarcinoma stem cells. Proc Natl Acad Sci USA 78, 7634-7638(1981).
3. Bradley, A. et al. Formation of germ-line chimaeras from embryo-derived teratocarcinoma cell lines. Nature 309, 255-256(1984).
4. Chambers, I. & Smith, A. Self-renewal of teratocarcinoma and embryonic stem cells. Oncogene 23, 7150-60(2004).
5. Rao, M. Conserved and divergent paths that regulate self-renewal in mouse and human embryonic stem cells. Developmental biology 275, 269-86(2004).
6. Murry, C.E. & Keller, G. Differentiation of embryonic stem cells to clinically relevant populations: lessons from embryonic development. Cell 132, 661-80(2008).
7. Olsen, A.L., Stachura, D.L. & Weiss, M.J. Designer blood: creating hematopoietic lineages from embryonic stem cells. Blood 107, 1265-75(2006).
8. Takahashi, K. & Yamanaka, S. Induction of pluripotent stem cells from mouse embryonic and adult fibroblast cultures by defined factors. Cell 126, 663–676 (2006).
9. Takahashi, K. et al. Induction of pluripotent stem cells from adult human fibroblasts by defined factors. Cell 131, 861–872 (2007).
10. Yu, J. et al. Induced pluripotent stem cell lines derived from human somatic cells. Science 318, 1917–1920 (2007).
11. Park, I. H. et al. Reprogramming of human somatic cells to pluripotency with defined factors.

Nature 451, 141–146 (2008).
12. Anokye-Danso, F. et al. Highly Efficient miRNA-Mediated Reprogramming of Mouse and Human Somatic Cells to Pluripotency. Cell stem cell 8, 376-88(2011).
13. Gonzàlez, F., Boué, S. & Belmonte, J.C.I. Methods for making induced pluripotent stem cells: reprogramming à la carte. Nature reviews. Genetics 12, 231-242(2011).
14. Chin, M.H. Induced pluripotent stem cells and embryonic stem cells are distinguished by gene expression signatures. Cell Stem Cell 5, 111-23(2009)
15. Kim, K. et al. Epigenetic memory in induced pluripotent stem cells. Nature 467, (2010).
16. Yamanaka, S. & Blau, H.M. Nuclear reprogramming to a pluripotent state by three approaches. Nature 465, 704-12(2010).
17. Ben-David, U. & Benvenisty, N. The tumorigenicity of human embryonic and induced pluripotent stem cells. Nature reviews. Cancer 11, 268-277(2011).
18. Pasi, C.E. et al. Genomic instability in induced stem cells. Cell Death and Differentiation 1-9(2011).
19. Lister, R. et al. Hotspots of aberrant epigenomic reprogramming in human induced pluripotent stem cells. Nature 470, 68-73(2011).
20. Osawa, M. et al. Long-term lymphohematopoietic reconstitution by a single CD34-low/negative hematopoietic stem cell. Science 273, 242-5(1996).
21. Bleyer, W. et al. Long-Term Remission From Acute Myelogenous Leukemia After Bone Marrow Transplantation and Recovery From Acute Graft-Versus-Host Reaction and Prolonged Immunoincompetence. Blood 45, 171(1975).
22. Verfaillie, C.M. Hematopoietic stem cells for transplantation. Nature immunology 3, 314-7(2002).
23. Keller, G. Embryonic stem cell differentiation: emergence of a new era in biology and medicine. Genes & development 19, 1129-55(2005).
24. Kyba, M. et al. HoxB4 confers definitive lymphoid-myeloid engraftment potential on embryonic stem cell and yolk sac hematopoietic progenitors. Cell 109, 29-37(2002).
25. Pilat, S. et al. HOXB4 enforces equivalent fates of ES-cell-derived and adult hematopoietic cells. Proc Natl Acad Sci USA 102, 12101-12106(2005).
26. Swiers, G., Bruijn, M. de & Speck, N. Hematopoietic stem cell emergence in the conceptus and the role of Runx1. The International journal of developmental biology 54, 1151-63(2010).
27. Orkin, S.H. & Zon, L.I. Hematopoiesis: an evolving paradigm for stem cell biology. Cell 132, 631-44(2008).
28. Lam, E.Y.N. et al. Live imaging of Runx1 expression in the dorsal aorta tracks the emergence of blood progenitors from endothelial cells. Blood 909-914(2010).
29. Boisset, J.-C. et al. In vivo imaging of haematopoietic cells emerging from the mouse aortic endothelium. Nature 464, 116-20(2010).
30. Bertrand, J.Y. et al. Haematopoietic stem cells derive directly from aortic endothelium during development. Nature 464, 108-11(2010).
31. Medvinsky, a, Rybtsov, S. & Taoudi, S. Embryonic origin of the adult hematopoietic system: advances and questions. Development 138, 1017-1031(2011).
32. Cumano, A. & Godin, I. Ontogeny of the hematopoietic system. Annual review of immunology 25, 745-85(2007).

33. Sabin, F.R. Studies on the origin of blood-vessels and of red blood-corpuscules as seen in the living blastoderm of chicks during the second day of gastrulation. Contributions to embryology 213-262(1920).
34. Sabin, F.R. On the origin of the cells of the blood. Physiological Reviews 2, 38(1922).
35. Ferkowicz, M.J. & Yoder, M.C. Blood island formation: longstanding observations and modern interpretations. Experimental hematology 33, 1041-7(2005).
36. Choi, K. The hemangioblast: a common progenitor of hematopoietic and endothelial cells. Journal of hematotherapy & stem cell research 11, 91-101(2002).
37. Choi, K., Kennedy, M., Kazarov, A., Papadimitriou, J. C. and Keller, G. A common precursor for hematopoietic and endothelial cells. Development 125,725-732(1998).
38. Huber, T.L. et al. Haemangioblast commitment is initiated in the primitive streak of the mouse embryo. Nature 432, 625-630(2004).
39. Fehling, H.J. Tracking mesoderm induction and its specification to the hemangioblast during embryonic stem cell differentiation. Development 130, 4217-4227(2003).
40. Herrmann, B. G. Expression pattern of the Brachyury gene in whole-mount TWis/TWis mutant embryos. Development 113, 913-917 (1991).
41. Kispert, A. & Herrmann, B. G. Immunohistochemical analysis of the Brachyury protein in wild-type and mutant mouse embryos. Dev. Biol. 161, 179-193(1994).
42. Kataoka, H. et al. Expressions of PDGF receptor alpha, c-Kit and Flk1 genes clustering in mouse chromosome 5 define distinct subsets of nascent mesodermal cells. Development, Growth and Differentiation 39, 729-740(1997).
43. Sakurai, H. et al. In vitro modeling of paraxial and lateral mesoderm differentiation reveals early reversibility. Stem cells 24, 575-86(2006).
44. Kattman, S.J. et al. Stage-Specific Optimization of Activin/Nodal and BMP Signaling Promotes Cardiac Differentiation of Mouse and Human Pluripotent Stem Cell Lines. Cell Stem Cell 8, 228-240(2011).
45. Park, C. et al. A hierarchical order of factors in the generation of FLK1- and SCL-expressing hematopoietic and endothelial progenitors from embryonic stem cells. Development 131, 2749-62(2004).
46. Lee, D. et al. ER71 acts downstream of BMP, Notch, and Wnt signaling in blood and vessel progenitor specification. Cell stem cell 2, 497-507(2008).
47. Yamaguchi, T.P. et al. Flk-1, an Flt-Related Receptor Tyrosine Kinase Is an Early Marker for Endothelial Cell Precursors. Development 118, 489-98(1993).
48. Shalaby, F. et al. A requirement for Flk1 in primitive and definitive hematopoiesis and vasculogenesis. Cell 89, 981-90(1997).
49. Shalaby, F., Rossant, J., Yamaguchi, T. P., Gertsenstein, M., Wu, X. F., Breitman, M. L., and Schuh, A. C. Failure of blood-island formation and vasculogenesis in Flk-1-deficient mice. Nature 376, 62-66 (1995)
50. Pimanda, J.E. et al. Gata2, Fli1, and Scl form a recursively wired gene-regulatory circuit during early hematopoietic development. PNAS 104, 17692-7(2007).
51. Nishikawa, S.-ichi et al. Progressive lineage analysis by cell sorting and culture identifies FLK1+VE-cadherin+ cells at a diverging point of endothelial and hemopoietic lineages. Development 125, 1747-57(1998).

52. Kallianpur, A. & Jordan, J. The SCL/TAL-1 gene is expressed in progenitors of both the hematopoietic and vascular systems during embryogenesis. Blood 83, 1200-1208(1994).
53. Takakura, N. et al. Critical role of the TIE2 endothelial cell receptor in the development of definitive hematopoiesis. Immunity 9, 677-86(1998).
54. Schnürch, H. & Risau, W. Expression of tie-2, a member of a novel family of receptor tyrosine kinases, in the endothelial cell lineage. Development 119, 957-68(1993).
55. Lancrin, C. et al. Blood cell generation from the hemangioblast. Journal of molecular medicine 88, 167-72(2010).
56. Ema, M. et al. Combinatorial effects of Flk1 and Tal1 on vascular and hematopoietic development in the mouse. Genes & development 17, 380-93(2003).
57. Drake, C.J. & Fleming, P. a Vasculogenesis in the day 6.5 to 9.5 mouse embryo. Blood 95, 1671-9(2000).
58. Samokhvalov, I.M., Samokhvalova, N.I. & Nishikawa, S.-I. Cell tracing shows the contribution of the yolk sac to adult haematopoiesis. Nature 446, 1056-61(2007).
59. Dzierzak, E. & Speck, N. Of lineage and legacy: the development of mammalian hematopoietic stem cells. Nature immunology 9, 129-36(2008).
60. England, S.J. et al. Immature erythroblasts with extensive ex vivo self-renewal capacity emerge from the early mammalian fetus. Blood 117, 2708(2011).
61. Lacaud, G. et al. Runx1 is essential for hematopoietic commitment at the hemangioblast stage of development in vitro. Blood 100, 458-66(2002).
62. Yokomizo, T. et al. Runx1 is involved in primitive erythropoiesis in the mouse. Blood 111, 4075-80(2008).
63. Eilken, H.M., Nishikawa, S.-I. & Schroeder, T. Continuous single-cell imaging of blood generation from haemogenic endothelium. Nature 457, 896-900(2009).
64. Huber, T.L. Dissecting hematopoietic differentiation using the embryonic stem cell differentiation model. The International journal of developmental biology 54, 991-1002(2010).
65. Mikkola, H.K.A. et al. Expression of CD41 marks the initiation of definitive hematopoiesis in the mouse embryo. 101, 508-516(2003).
66. Taoudi, S. et al. Progressive divergence of definitive haematopoietic stem cells from the endothelial compartment does not depend on contact with the foetal liver. Development 132, 4179-91(2005).
67. Burns, C.E. et al. Hematopoietic stem cell fate is established by the Notch-Runx pathway. Genes & development 19, 2331-42(2005).
68. Chen, M.J. et al. Runx1 is required for the endothelial to haematopoietic cell transition but not thereafter. Nature 457, 887-91(2009).
69. North, T.E. et al. Runx1 expression marks long-term repopulating hematopoietic stem cells in the midgestation mouse embryo. Immunity 16, 661-72(2002).
70. Okuda, T. et al. AML1, the target of multiple chromosomal translocations in human leukemia, is essential for normal fetal liver hematopoiesis. Cell 84, 321-30(1996).
71. Attisano, L. & Wrana, J.L. Signal transduction by the TGF-beta superfamily. Science 296, 1646-7(2002).
72. Thatcher, J.D. The TGF-beta signal transduction pathway. Science signaling 3, tr4(2010).
73. Derynck, R. & Zhang, Y.E. Smad-dependent and Smad-independent pathways in TGF-beta

family signalling. Nature 425, 577-84(2003).
74. Sadlon, T.J., Lewis, I.D. & D'Andrea, R.J. BMP4: Its Role in Development of the Hematopoietic System and Potential as a Hematopoietic Growth Factor. Stem Cells 22, 457-474(2004).
75. Decaestecker, M. The transforming growth factor-β superfamily of receptors. Cytokine & Growth Factor Reviews 15, 1-11(2004).
76. Winnier, G. et al. Bone morphogenetic protein-4 is required for mesoderm formation and patterning in the mouse. Genes & development 9, 2105-16(1995).
77. Nakayama, N., Lee, J. & Chiu, L. Vascular endothelial growth factor synergistically enhances bone morphogenetic protein-4-dependent lymphohematopoietic cell generation. Blood 95, 2275(2000).
78. Pimanda, J.E. et al. The SCL transcriptional network and BMP signaling pathway interact to regulate RUNX1 activity. PNAS 104, 840-5(2007).
79. Lengerke, C. et al. BMP and Wnt Specify Hematopoietic Fate by Activation of the Cdx-Hox Pathway. Cell stem cell 2, 72-82(2008).
80. Robin, C. & Durand, C. The roles of BMP and IL-3 signaling pathways in the control of hematopoietic stem cells in the mouse embryo. International Journal 1200, 1189-1200(2010).
81. Chiang, P.-M. & Wong, P.C. Differentiation of an embryonic stem cell to hemogenic endothelium by defined factors: essential role of bone morphogenetic protein 4. Development 2843, 2833-2843(2011).
82. Snyder, A., Fraser, S.T. & Baron, M.H. Bone morphogenetic proteins in vertebrate hematopoietic development. Journal of cellular biochemistry 93, 224-32(2004).
83. Zafonte BT, Liu S, Lynch-Kattman M, et al. Smad1 expands the hemangioblast population within a limited developmental window. Blood. (2007)
84. Cook, B.D., Liu, S. & Evans, T. Smad1 signaling restricts hematopoietic potential after promoting hemangioblast commitment. Blood (2011).
85. Liu, P., Wakamiya, M., Shea, M.J., Albrecht, U., Behringer, R.R.,Bradley, A. Requirement for Wnt3 in vertebrate axis formation. Nat. Genet. 22, 361—365(1999)
86. Kelly, O.G., Pinson, K.I., Skarnes, W.C. The Wnt co-receptors Lrp5 and Lrp6 are essential for gastrulation in mice. Development 131, 2803—2815(2004).
87. Huelsken, J., Vogel, R., Brinkmann, V., Erdmann, B., Birchmeier, C., Birchmeier, W. Requirement for beta-catenin in anteriorposterior axis formation in mice. J. Cell Biol. 148, 567—578(2000)
88. Wang, Y. & Nakayama, N. WNT and BMP signaling are both required for hematopoietic cell development from human ES cells. Stem Cell Research 3, 113-125(2009).
89. Pilon, N. et al. Wnt signaling is a key mediator of Cdx1 expression in vivo. Development 134, 2315-23(2007).
90. Pilon, N. et al. Cdx4 is a direct target of the canonical Wnt pathway. Developmental biology 289, 55-63(2006).
91. Lengerke, C. et al. The cdx-hox pathway in hematopoietic stem cell formation from embryonic stem cells. Annals of the New York Academy of Sciences 1106, 197-208(2007).
92. Helgason, C.D. et al. Overexpression of HOXB4 enhances the hematopoietic potential of embryonic stem cells differentiated in vitro. Blood 87, 2740-9(1996).

93. Kyba, M., Perlingeiro, R.C.R. & Daley, G.Q. HoxB4 confers definitive lymphoid-myeloid engraftment potential on embryonic stem cell and yolk sac hematopoietic progenitors. Cell 109, 29-37(2002).
94. Davidson, A.J. & Zon, L.I. The caudal-related homeobox genes cdx1a and cdx4 act redundantly to regulate hox gene expression and the formation of putative hematopoietic stem cells during zebrafish embryogenesis. Developmental biology 292, 506-18(2006).
95. Davidson, A.J. et al. Cdx4 Mutants Fail To Specify Blood Progenitors and Can Be Rescued By Multiple Hox Genes. Nature 425, 300-6(2003).
96. MacDonald, B.T., Tamai, K. & He, X. Wnt/beta-catenin signaling: components, mechanisms, and diseases. Developmental cell 17, 9-26(2009).
97. Hirashima, M. et al. Maturation of embryonic stem cells into endothelial cells in an in vitro model of vasculogenesis. Blood 93, 1253-63(1999).
98. Yamashita, J.K. et al. Flk1-positive cells derived from embryonic stem cells serve as vascular progenitors. Nature 408, (2000).
99. Hirashima, M. et al. A chemically defined culture of VEGFR2+ cells derived from embryonic stem cells reveals the role of VEGFR1 in tuning the threshold for VEGF in developing endothelial cells. Blood 101, 2261(2003).
100. Ferdous, A., Caprioli, A. & Iacovino, M. Nkx-5 transactivates the Ets-related protein 71 gene and specifies an endothelial/endocardial fate in the developing embryo. PNAS (2009).
101. Sumanas, S. & Lin, S. Ets1-related protein is a key regulator of vasculogenesis in zebrafish. PLoS biology 4, e10(2006).
102. Sumanas, S. et al. Interplay among Etsrp/ER71, Scl, and Alk8 signaling controls endothelial and myeloid cell formation. Blood 111, 4500-10(2008).
103. Dumont, D. J., et al. Tek, a novel tyrosine kinase gene located on mouse chromosome 4, is expressed in endothelial cells and their presumptive precursors. Oncogene 7, 1471-1480 (1992)
104. Sato, T.N. et al. Tie-1 and tie-2 define another class of putative receptor tyrosine kinase genes expressed in early embryonic vascular system. PNAS 90, 9355-8(1993).
105. Kisanuki, Y.Y. et al. Tie2-Cre transgenic mice: a new model for endothelial cell-lineage analysis in vivo. Developmental biology 230, 230-42(2001).
106. Hamaguchi, I. et al. In vitro hematopoietic and endothelial cell development from cells expressing TEK receptor in murine aorta-gonad-mesonephros region. Blood 93, 1549-56(1999).
107. Dumont D.J. et al. Dominant-negative and targeted null mutations in the endothelial receptor tyrosine kinase, tek, reveal a critical role in vasculogenesis of the embryo. Genes Dev 8:1897, (1994)
108. Lamb, T.J., Graham, A.L. & Petrie, A. T testing the immune system. Immunity 28, 288-92(2008).
109. Nishikawa, S. et al. Stromal cell-dependent bone marrow culture with a nearly protein-free defined medium. Immunology letters 40, 163-9(1994).
110. Boergermann, J.H. et al. Dorsomorphin and LDN-193189 inhibit BMP-mediated Smad, p38 and Akt signalling in C2C12 cells. The international journal of biochemistry & cell biology 42, 1802-1807(2010).
111. Huang, S.-M. a et al. Tankyrase inhibition stabilizes axin and antagonizes Wnt signalling. Nature 461, 614-20(2009).

112. Arthur, H.M. et al. Endoglin, an ancillary TGFbeta receptor, is required for extraembryonic angiogenesis and plays a key role in heart development. Developmental biology 217, 42-53(2000).
113. Jonker, L. & Arthur, H.M. Endoglin expression in early development is associated with vasculogenesis and angiogenesis. Mechanisms of Development 110, 193-196(2002).
114. Baldwin, H.S. et al. Platelet endothelial cell adhesion molecule-1 (PECAM-1/CD31): alternatively spliced, functionally distinct isoforms expressed during mammalian cardiovascular development. Development 120, 2539-53(1994).
115. Pearson, S. et al. The sequential expression of CD40 and Icam2 defines progressive steps in the formation of blood precursors from the mesoderm germ layer. Stem cells 28, 1089-98(2010).
116. Wilson, N.K. et al. Combinatorial Transcriptional Control In Blood Stem/Progenitor Cells: Genome-wide Analysis of Ten Major Transcriptional Regulators. Cell stem cell 7, 532-44(2010).
117. Lugus, J.J. et al. GATA2 functions at multiple steps in hemangioblast development and differentiation. Development 134, 393-405(2007).
118. Birdsey, G.M. et al. Transcription factor Erg regulates angiogenesis and endothelial apoptosis through VE-cadherin. Blood 111, 3498-506(2008).
119. Hromas, R. et al. Hematopoietic lineage- and stage-restricted expression of the ETS oncogene family member PU.1. Blood 82, 2998-3004(1993).
120. Yamamoto, M. et al. Upstream and downstream of erythroid transcription factor GATA-1. Genes to cells : devoted to molecular & cellular mechanisms 2, 107-15(1997).
121. Soriano, P. Generalized lacZ expression with the ROSA26 Cre reporter strain. Nature genetics 21, 70-1(1999).
122. Boer, J. de et al. Transgenic mice with hematopoietic and lymphoid specific expression of Cre. European journal of immunology 33, 314-25(2003).
123. Liao, W.P. et al. Generation of a mouse line expressing Sox17-driven Cre recombinase with specific activity in arteries. Genesis 47, 476-83(2009).
124. Saga, Y. et al. MesP1 is expressed in the heart precursor cells and required for the formation of a single heart tube. Development 126, 3437-47(1999).
125. Sauer, B. Inducible gene targeting in mice using the Cre/lox system. Methods: A Companion to Methods in Enzymology 14, 381-92(1998).
126. Fraser, S.T. et al. Putative intermediate precursor between hematogenic endothelial cells and blood cells in the developing embryo. Development, growth & differentiation 45, 63-75(2003).
127. Gomez, G.A. et al. Discovery and characterization of novel vascular and hematopoietic genes downstream of etsrp in zebrafish. PloS one 4, e4994(2009).
128. Wong, K.S. et al. Identification of vasculature-specific genes by microarray analysis of Etsrp/Etv2 overexpressing zebrafish embryos. Developmental dynamics. 238, 1836-50(2009).
129. Friedman, A.D. Cell cycle and developmental control of hematopoiesis by Runx1. Journal of cellular physiology 219, 520-4(2009).
130. Hayward, P., Kalmar, T. & Arias, A.M. Wnt/Notch signalling and information processing during development. Development 135, 411-24(2008).

8. Abbreviations used

Abbreviation	*Meaning*
2-ME	2-Mercaptoethanol
APC	Allophycocyanin
BFU-E	Burst-Forming Unit-Erythroid
BMP	Bone Morphogenic Protein
Bry	Brachyury
BSA	Bovine Serum Albumin
CFU	Colony-Forming Unit
CFU-G	CFU-Granulocyte
CFU-GEMM	CFU-Granulocyte, Erythroid, Macrophage, Megakaryocyte
CFU-GM	CFU-Granuolcyte, Macrophage
CFU-M	CFU-Macrophage
Co-Smad	Common-Smad
Cre	Cre-Recombinase
DNA	Deoxyribose Nucleic Acid
dpc	day post-coitum
Dvl	Dishvelled
E	Embryonic day
ES	Embryonic Stem
Etsrp	Ets-related protein
Etv2	Ets variant 2
FACS	Fluorescence-Activated Cell Sorting
FITC	Fluorescein Isothiocyanate
Flk1	Fetal liver kinase 1
Fz	Frizzled
G-CSF	Granulocyte-Colony-Stimulating Factor
HBSS	Hank's balanced salt solution
HDAC	Histone Deacetylase
HSC	Hematopoietic Stem Cell
ICAM2	Intercellular Adhesion Molecule 2

iPS	induced Pluripotent Stem
KO-DMEM	Knock-out Dulbecco's Modified Eagle's Medium
mIL	mouse Interleukin
min	minute
MoAb	Monoclonal Antibody
NEAA	Non-Essential Amino Acids
PBS	Phosphate-Buffered Saline
PCR	Polymerase Chain Reaction
PDGFRα	Platelet-Derived Growth Factor Receptor α
PE	Phycoerythrin
PECAM-1	Platelet Endothelial Cell Adhesion Molecule 1
PI	Prodidium Iodide
qRT-PCR	quantitative Reverse Transcriptase-PCR
R-Smad	Receptor-activated Smad
rhEPO	recombinant human Erythropoietin
rmEPO	recombinant mouse Erythropoietin
RNA	Ribose Nucleic Acid
RT	Room Temperature
Runx1	Runt-related transcription factor 1
SCF	Stem Cell Factor
sec	second
SEM	Standard Error of the Mean
TGF-β	Transforming Growth Factor-β
TNKS	Tankyrase
VE-Cad	Vascular Endothelial Cadherin
VEGF	Vascular Endothelial Growth Factor
VEGFR	Vascular Endothelial Growth Factor Receptor
αMEM	α-Minimal Essential Medium